Supporting Information for:

Cooperatively Designed Aptamer-PROTACs for Spatioselective Degradation of Nucleocytoplasmic Shuttling Protein for Enhanced Combinational Therapy

Ran Liu [a], *Zheng Liu* [a], *Mohan Chen* [a], *Hang Xing* [b], *Penghui Zhang* [c,*], *and Jingjing Zhang* [a,*]

[a]State Key Laboratory of Analytical Chemistry for Life Science, School of Chemistry and Chemical Engineering, Chemistry and Biomedicine Innovation Center (ChemBIC), Nanjing University, Nanjing 210023, China.

[b]Institute of Chemical Biology and Nanomedicine, State Key Laboratory of Chemo/Biosensing and Chemometrics, Hunan Provincial Key Laboratory of Biomacromolecular Chemical Biology, College of Chemistry and Chemical Engineering, Hunan University, Changsha 410082, China.

[c]Zhejiang Cancer Hospital, The Key Laboratory of Zhejiang Province for Aptamers and Theranostics, Hangzhou Institute of Medicine (HIM), Chinese Academy of Sciences, Hangzhou 310022, China

*Corresponding author. E-mail addresses: phzhang@ucas.ac.cn (P. Zhang), jing15209791@nju.edu.cn (J. Zhang).

Supplementary Text

Section A: Materials and reagents

All oligonucleotides used in this study were synthesized by Shanghai Sangon Biological Engineering Co., Ltd. (Shanghai, China) and purified by HPLC. The detailed sequences are shown in Table S1. For stock solution preparation, all DNA sequences were dissolved and diluted with Millipore water to a final concentration of 20 μM. After annealing for 5 min at 90°C, the resulting solutions were cooled down to room temperature and stored at 4℃ until use.

High Precision Streptavidin-2 biosensors (Fortebio) were purchased from FroteBio (Menlo Park, CA, USA). Recombinant Human CUL4A/RBX1/DDB1/CRBN Complex Protein (E3-650-025) were provided by R&D Systems (Minneapolis, USA). Recombinant Human Nucleolin (RPC242Hu01) were purchased from Cloud-clone Corp (Wuhan, China). Total RNA Purification Kit (B511361), High sensitive ECL luminescence reagent (C500044) and Cell Counting Kit-8 (CCK-8, E606335) were provided by Shanghai Sangon Biological Engineering Co., Ltd. (Shanghai, China). Anti-Nucleolin antibody (ab129200) and Anti-Histone H3 antibody (ab32356) were purchased from Abcam (Shanghai, China). β-Actin Rabbit mAb (8457S) and Estrogen Receptor alpha Rabbit mAb (8644S) was purchased from Cell Signaling Technology, Inc. (Shanghai,China). MLN4924 (S81085) were purchased from Shanghai yuanye Bio-Technology Co., Ltd (Shanghai, China). 4-fluoroisobenzofuran-1,3-dione (467707) and 14-azido-3,6,9,12-tetraoxatetradecan-1-amine (901138) were provided by Shanghai Macklin Biochemical Co., Ltd. The pomalidomide-PEG4-azide (HY-141015), pomalidomide-PEG1-azide (HY-133138), (S,R,S)-AHPC-PEG3-N3 (HY-103598) and 3-Amino-1-methylpiperidine-2,6-dione hydrochloride (HY-W225136A) were purchased from MedChemExpress LLC (Shanghai,China). Zeba™ Spin Desalting Columns (89892), NE-PER extraction reagents (78835) and Halt™ Protease Inhibitor Cocktail, EDTA-Free (87785) were provided by Thermo Fisher Scientific (USA). CytoTraceTM red fluorescent probe was purchased from Yeasen Biological Technology (Shanghai, China). The Cell Cycle Detection Kit (KGA512) was purchased from KeyGEN BioTECH (Jiangsu, China). The FITC Annexin V Apoptosis Detection Kit (556547) was provided by BD Pharmingen™ (USA). PrimeScriptTM RT reagent Kit (RR047A) and TB Green® Premix Ex Taq™ (RR420A) were purchased from Takara Biomedical Technology Co., Ltd. (Beijing, China). T4 DNA ligase (M0202S) was purchased from New England Biolabs (Beijing, China) Ltd. Specific-pathogen-free female BALB/c nude mice (5-6 weeks old) were purchased from the Changzhou Cavens Laboratory Animal Ltd, and used according to the regulations of the Institutional Animal Care and Use Committee of Nanjing University (animal protocol number: IACUC-2204009). Othe reagents (analytical grade) were purchased from Sinopharm Chemical Reagent Co.(Shanghai, China). All solutions were prepared with Millipore water (18.25 MΩ·cm-1).

Buffers used in this work:

5X click buffer: 1500 mM NaCl, 50 mM Tris, 5 mM EDTA, pH 7.5.

DPBS buffer: 137 mM NaCl, 2.7 mM KCl, 8.1 mM Na_2HPO_4, 1.47 mM KH_2PO_4,0.9 mM $CaCl_2$, 0.49 mM $MgCl_2$, pH 7.4.

0.5X TBE buffer: 4.5 mM Tris, 4.5 mM boric acid, 0.1 mM EDTA, pH 8.2.

Section B: Experimental details

Section B1. Preparation and characterization of PS-ApTCs.

Synthesis and mass characterization of PS-ApTCs. The PS-ApTCs was synthesized through a copper-free click reaction by conjugating azide-modified pomalidomide to DBCO-modified PS-AS1411. Briefly, a click reaction solution was prepared by mixing 375 μL of DBCO-modified DNA oligonucleotides (20 μM), 15 μL of pomalidomide-PEG4-azide (10 mM), 120 μL of 5X click buffer and 90 μL of Millipore water. After vortexing for 30 s, the reaction mixture was then placed on a shaker for 16 h at 37°C. The resulting mixture was purified using spin desalting columns (Zeba™ 7K MWCO, Thermo Fisher) to remove unconjugated pomalidomide-PEG4-azide. Finally, the concentration of purified PS-ApTCs was quantified with a NanoDrop Onec (Thermo Fisher). Following the same protocol, ApTCs, ApTCs-Biotin, PS-ApTCs-Biotin, Random-PROTACs (R-PROTACs), PS-ApTCs-Cy5, PS-ApTCs-FAM and R-PROTACs-Cy5 were prepared using DBCO-AS1411, DBCO-AS1411-Biotin, DBCO-AS1411-PS-Biotin, DBCO-Random-PS, DBCO-AS1411-PS-Cy5, DBCO-AS1411-PS-FAM and DBCO-Random-PS-Cy5, respectively. All the above compounds were diluted to a final working concentration of 100 μM. PS-ApTCs-PEG1 were synthesized through a copper-free click reaction by conjugating azide-modified pomalidomide with 1-polyethylene glycols (PEGs) linker to DBCO-modified PS-AS1411.

DBCO-AS1411-PS and PS-ApTCs were characterized using MALDI-TOF mass spectrometry, which was recorded on an ABI-MDS SCIEX 4800 Plus MALDI TOF/TOF™ mass spectrometer.

Serum stability assay of PS-ApTCs. The serum stability assay of PS-ApTCs was assessed by mixing 2 μL fresh fetal bovine serum, 2 μL PS-ApTCs (10 μM), and 16 μL Millipore water. After incubation at 37°C for up to 24 h, the resulting mixture was immediately analyzed using 8% native polyacrylamide gel electrophoresis (nPAGE) with the following experimental conditions: voltage (80 V), 0.5X TBE buffer, 80 min. The band intensity was quantitated by Image J. For comparison, ApTCs was used as a negative control and analyzed following the same protocol as above.

Synthesis and characterization of azide-modified N-methyl pomalidomide and Control-PS-ApTCs. The azide-modified N-methyl pomalidomide was synthesized according to the previous reports.[1,2] The general synthetic scheme for the azide-modified N-methyl pomalidomide is depicted in Fig. S10.

Compound 3: *4-Fluoro-2-(1-methyl-2,6-dioxo-3-piperidyl)isoindoline-1,3-dione*

A mixture of the 3-fluoroisobenzofuran-1,3-dione (1.5 eq., 1.5 mmol) and 3-amino-1-methylpiperidine-2,6-dione hydrochloride (1.0 eq., 1 mmol) and a solution of sodium acetate (100 mg, 1.2 mmol) in glacial acetic acid (10 mL) was refluxed for 6 h at 125°C. After cooling, it was poured onto H_2O (50 mL) and the solid formed was collected by filtration, washed with H_2O (3×5 mL) and petroleum ether (3×5 mL), and dried in vacuo. Yield: 0.2020 g, 0.7 mmol (63%).

Compound 5: *4-((14-azido-3,6,9,12-tetraoxatetradecyl)amino)-2-(1-methyl-2,6-dioxopiperidin-3-yl)isoindoline-1,3-dione*

A mixture of 14-azido-3,6,9,12-tetraoxatetradecan-1-amine (1.1 eq., 0.55 mmol), compound 3 (1.0 eq., 0.5 mmol) and N,N-Diisopropylethylamine (DIPEA, 0.13 g, 0.17 mL, 1.0 mmol) in dry N,N-Dimethylformamide (DMF, 10 mL) was stirred at 93°C for 10 h. The mixture was cooled to roomtemperature, poured into H_2O (100 mL) and extracted with EtOAc (3×50 mL). The combined organic layers were washed with H_2O (50 mL) and brine (50 mL), dried over Na_2SO_4, filtered and concentrated in vacuo. The crude product was purificated by column chromatography (gradient of petroleum ether /EtOAc 4:1 to 1:2) to obtain compound 5. Yield: 0.0847 g, 0.16 mmol (32%).

^{1}H-, ^{13}C-NMR spectra were acquired on a Bruker DRX-500 spectrometer at 25°C. Chemical shifts are reported in parts per million (ppm, δ) downfield from tetramethylsilane (TMS). Coupling constants (*J*) are reported in Hz. Spin multiplicities are described as br (broad), s (singlet), d (doublet), t (triplet), q (quartet), m (multiplet). Mass spectroscopy analysis was performed using a LTQ-Orbitrap XL mass spectrometer (ThermoFisher).

Control-PS-ApTCs was synthesized through a copper-free click reaction by conjugating azide-modified N-methyl pomalidomide to DBCO-modified PS-AS1411. The qPCRs procedure is the same as described in Section B1. Mass analysis was performed on a Thermo LTQ Orbitrap XL mass spectrometer. The source voltage was set at 4500 V with a heated capillary temperature of 350°C.

Bio-layer interferometry characterization of PS-ApTCs. Bio-layer interferometry (BLI) experiments were conducted using an Octet K2 instrument (FroteBio) equipped with High Precision Streptavidin-2 Biosensors. Briefly, 1) to investigate the binding property of PS-ApTCs binding to nucleolin, PS-ApTCs-Biotin (50 nM) immobilized BLI sensor was incubated with 200 nM nucleolin, and association and dissociation rates were measured by the shift in wavelength (nm). All reactions were performed at 30°C in DPBS. For comparison, ApTCs-Biotin (50 nM) was used as a control and analyzed following the same protocol as above. 2) To measure the equilibrium dissociation constant (K_D) of PS-ApTCs binding to nucleolin and CRBN, PS-ApTCs-Biotin (300 nM) immobilized BLI sensor was incubated with different concentrations of nucleolin (25-300 nM) and CRBN (5-50 nM), respectively. 3) Ternary complex formation between CRBN, nucleolin and PS-ApTCs was investigated by successive incubating the PS-ApTCs-Biotin (100 nM) immobilized BLI sensor in 30 nM CRBN and 200 nM nucleolin solutions.

The experimental procedure for the ternary complex formation between CRBN, nucleolin and other PROTACs is similar to the one mentioned above except that the PS-ApTCs-Biotin was replaced by PS-ApTCs-PEG1-Biotin or Control-PS-ApTCs-Biotin.

All BLI data were analyzed using FroteBio Octet analysis software and the K_D was estimated by fitting of the obtained BLI data to a 1:1 binding model. "R" indicates the practical signals from the sample measurement, and "R_t" represents the signals at the end of regeneration. "R_{eq}" is the equilibrium signal at a certain analyte concentration. The binding constant are derived as follow:

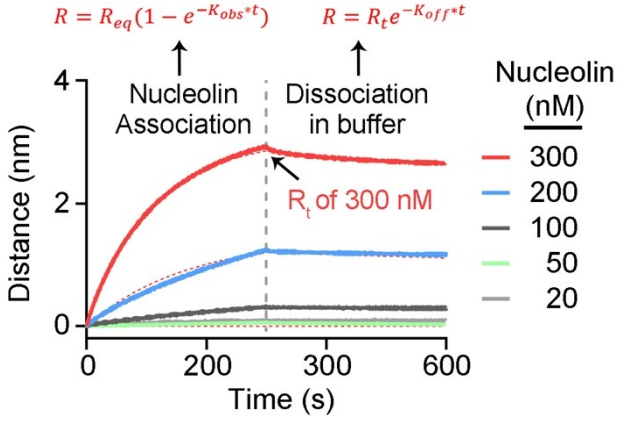

The equilibrium dissociation constant (K_D) is a measure of how tightly a ligand binds to a receptor or target protein. It is calculated as the ratio of the dissociation rate constant (K_{off}) to the association rate constant (K_{on}):

$$K_D = \frac{K_{off}}{K_{on}}$$

The K_{off} represents the speed at which the target protein dissociates from the ligand, while the K_{on} represents the speed at which the ligand binds to the protein. The K_{on} can be calculated by measuring the observed rate constant (K_{obs}) and the ligand concentration [Conc (M)], using the equation:

$$K_{on} = \frac{K_{obs} - K_{off}}{[Conc\ (M)]}$$

The observed rate constant (K_{obs}) can be determined from experimental data using the equation:

$$R = R_{eq}(1 - e^{-K_{obs} * t})$$

The dissociation rate constant (K_d) can also be determined experimentally, using the equation:

$$R = R_t e^{-K_{off} * t}$$

Section B2. Procedure for spatioselective degradation of nucleolin in target cells using PS-ApTCs.

Cancer cell-targeting study of PS-ApTCs. Human cervical cancer cells (HeLa) were cultured in complete DMEM medium that was prepared to contain 10% fetal bovine serum, 80 U/mL penicillin, and 80 μg/mL streptomycin. Human normal hepatocytes (L-02) were cultured in a RPMI-1640 medium supplemented with 10% fetal bovine serum, 80 U/mL penicillin, and 80 μg/mL streptomycin. All cells in culture medium were kept at 37℃ in a humidified incubator with 5% CO_2.

For confocal microscopic imaging, HeLa cells or L-02 cells were seeded onto 20 mm round glass coverslips placed in 12-well plates and grown until it reached 70-80% confluency. After that, the cells were washed three times with DPBS buffer, and subsequently incubated with 500 μL FAM-labeled PS-ApTCs (200 nM) in DPBS for 60 min at 4℃. Then, the cells were washed three times with DPBS buffer and fixed in 4% polyformaldehyde for 15 min. Before confocal imaging, the cell nuclei were first stained with 500 μL Hoechst 33342 solution (12.5 μg/mL) for 15 min, and then washed three times with DPBS buffer. Finally, the coverslip was sealed to a slide with an anti-fluorescence quenching agent, and subjected to imaging using a Leica SP8 laser scanning confocal microscope (Leica, Germany). The excitation wavelengths were 405 and 488 nm for Hoechst and FAM, respectively. For comparison, FAM-AS1411 was used as a control and analyzed following the same protocol as above.

For flow cytometric analysis, HeLa cells or L-02 cells were first cultured in 6-well plates, and grown until it reached 70-80% confluency. After that, the cells were washed three times with DPBS buffer, and subsequently digested with 0.25% trypsin (1000 μL) for 10 min at 37℃. Then, the resulting cells were collected and incubated with 1000 μL FAM-labeled PS-ApTCs (200 nM) in DPBS for 60 min at 4℃, followed by washing with DPBS buffer. Finally, flow cytometric analysis of cells (10,000 cells per sample) was conducted using a CytoFlex flow cytometry system (Beckman Coulter Inc., USA), with excitation at 488 nm and emission at 525 nm. Untreated cells were used as negative control. For comparison, FAM-AS1411 was used as a control and analyzed following the same protocol as above.

Time-dependent internalization and intracellular localization study of PS-ApTCs. HeLa cells were seeded onto 20 mm round glass coverslips placed in 12-well plates and grown until it reached 70-80% confluency. After that, the cells were washed three times with DPBS buffer, and subsequently incubated with 500 μL FAM-labeled PS-ApTCs (200 nM) in DPBS at 37℃ for different times up to 240 min. Then, the cells were successively treated with CytoTrace red fluorescent probe (500 μL, 1X) for cytoplasm staining and Hoechst 33342 (500 μL, 12.5 μg/mL) for nuclei staining. Finally, the coverslip was sealed to a slide with an anti-fluorescence quenching agent, and subjected to imaging using a Leica SP8 laser scanning confocal microscope (Leica, Germany). The excitation wavelengths were 405, 488, and 577 nm for Hoechst, FAM, and CytoTrace, respectively. Mander's overlap colocalization coefficient (MOC) quantifying the degree of colocalization of the two fluorescence signals was calculated by analysing more than 10 cells of each sample using the Image J software.

Confocal microscopic imaging of nucleolin in cell membranes after PS-ApTCs treatment. Firstly, HeLa cells were first cultured in 12-well plates, and grown until it reached 70-80% confluency. After that, the cells were washed three times with DPBS buffer, and subsequently incubated with 500 μL PS-ApTCs (200 nM) in complete DMEM medium for different times up to 24 h. Then, the cell nuclei were stained with 500 μL Hoechst 33342 solution (12.5 μg/mL) for 15 min. After that, the cells were washed three times with DPBS buffer, and subsequently digested with 0.25% trypsin (500 μL) for 10 min at 37℃. The resulting cells were collected and incubated with 500 μL FAM-AS1411 (200 nM) in DPBS for 60 min at 4℃. Before confocal imaging, the cells were washed twice with DPBS, centrifuged at 1000 rpm for 3 minutes, and then resuspended in 100 μL of DPBS. Finally, 10 μL of cell suspension were dropped on a 20-mm glass-bottom culture dish (NEST Biotechnology, China) and subjected to imaging using a Leica SP8 laser scanning confocal microscope (Leica, Germany). The excitation wavelengths were 405 and 488 nm for Hoechst and FAM, respectively. Untreated cells (NT), R-PROTACs, and PS-AS1411 were also applied as controls and analyzed following the same protocol as above.

Flow cytometric analysis of nucleolin in cell membranes after PS-ApTCs treatment. For flow cytometric analysis, HeLa cells were first cultured in 6-well plates, and grown until it reached 70-80% confluency. After that, the cells were washed three times with DPBS buffer, and subsequently incubated with 1000 μL PS-ApTCs (200 nM) in complete DMEM medium for different times up to 24 h. After that, the cells were washed three times with DPBS buffer, and subsequently digested with 0.25% trypsin (1000 μL) for 10 min at 37℃. Then, the resulting cells were collected and incubated with 1000 μL FAM-AS1411 (200 nM) in DPBS for 60 min at 4°C, followed by washing with DPBS buffer. Finally, flow cytometric analysis of cells (10,000 cells per sample) was conducted using a CytoFlex flow cytometry system (Beckman Coulter Inc., USA), with excitation at 488 nm and emission at 525 nm. Untreated cells (NT), R-PROTACs, and PS-AS1411 were also applied as controls and analyzed following the same protocol as above.

Immunoblots analysis of nucleolin in cytoplasm and nucleus after PS-ApTCs treatment. To detect the effect of PS-ApTCs on the level of nucleolin protein in cytoplasm and nucleus, HeLa cells were first cultured in 6-well plates, and grown until it reached 70-80% confluency. After that, the cells were washed three times with DPBS buffer, and subsequently treated with 1000 μL of 200 nM PS-ApTCs, PS-AS1411, or PS-ApTCs/PS-AS1411 for 24 h, respectively. Then, cytoplasmic and nuclear extracts of the resulting cells were prepared using the NE-PER extraction reagents from Thermo, according to manufacturer's instructions. Before Western blotting analysis, the total protein concentration was determined and normalized using a BCA protein assay kit (Shanghai Sangon Biotech, C503021). Finally, the nucleolin levels in cytoplasm and nuclear were

analyzed by standard Western blotting with indicated antibodies. β-actin and histone was used as the cytoplasmic and nuclear protein control, respectively. For proteasome inhibition study, HeLa cells were treated with 200 nM MG132 for 24 h prior to incubation with 200 nM PS-ApTCs. The symbols "+" and "-", indicate the presence and absence of the corresponding molecules, respectively. The Western blotting images were obtained by Tanon-4600 Chemiluminescent Imaging System (Tanon, China). Quantification of Western blot bands was performed using Image J software. All protein levels were normalized to β-actin or histone prior to comparison between experimental conditions.

For the time-course degradation experiments, HeLa cells were treated with 200 nM PS-ApTCs for up to 48 h, and the cytoplasmic nucleolin levels were analyzed following the same protocol as above. Untreated HeLa cells were used as negative controls.

For the dose-dependent degradation experiments, HeLa cells were treated with different concentrations of PS-ApTCs or Control-PS-ApTCs (0.1-1000 nM) for 24 h, and the cytoplasmic nucleolin levels were analyzed following the same protocol as above. Median degradation concentration (DC_{50}) of immunoblots analysis is calculated with Image J software.

MS-based proteomics analysis of PS-ApTCs. 1) Sample preparation. HeLa cells were first cultured in T-25 culture flask, and grown until it reached 70-80% confluency. After that, the cells were washed three times with DPBS buffer, and subsequently treated with 4000 μL of 200 nM PS-ApTCs or PS-AS1411 for 24 h, respectively. Then, cytoplasmic extracts of the resulting cells were prepared using the NE-PER extraction reagents from Thermo, according to manufacturer's instructions. A total of 10 μg protein per sample were labeled with isotopic dimethylation reagents were labeled with isotopic dimethylation reagents using in-solution procedures as previously described.[3] Trypsin-digested peptides from PS-ApTCs and PS-AS1411 treated groups were labeled with CH_2O and CD_2O dimethyl isotopes, respectively. The samples were then desalted using a C18 SPE cartridge column (87784, Thermo Fisher) as per the manufacturer's instructions. After labeling, the peptides from the two samples were pooled together in equal proportions. **2) Liquid chromatography–tandem mass spectrometry analysis.** The pooled sample was fractionated using low-pH reverse-phase chromatography on an EASY-nLC 1200 nano-UHPLC coupled to Q-Exactive HF-X Quadrupole-Orbitrap mass spectrometer (Thermo Scientific). The mobile phase consisted of 0.1% formic acid in deionized water (mobile phase A) and 0.1% formic acid in acetonitrile (mobile phase B). The flow was maintained at 300 μL per minute through the following gradient: 3–5% mobile phase B in 0–5 s, 5–15% mobile phase B in 5 s–53.60 min, 15–28% mobile phase B in 53.60–100.25 min, 28–38% mobile phase B in 100.25–116.92 min; Finally, within 5 seconds, solution B was increased to 100% and maintained for 8 minutes. To generate MS/MS spectra, MS1 spectra (scan range = 350–1800 m/z) were first acquired in the Orbitrap mass analyzer with a resolution of 60,000. Peptide precursor ions were isolated and fragmented using high-energy collision-induced dissociation (HCD). The resulting MS/MS fragmentation spectra were acquired in the ion trap. The 20 most intense precursor ions were sequentially fragmented by higher-energy collision dissociation. MS2 resolution was set at 15,000. The normalized collision energy was set at 28%. The maximum ion injection times for MS1 and MS2 were set at 50 ms. **3) Peptide and protein identification.** The raw mass spectrometry data files were searched against the Uniprot-sprot-Human-Canonical database by MaxQuant software v.1.6.5.0 for protein identification and dimethyl reporter quantitation. The following MaxQuant parameters were used: enzyme used, trypsin/P; maximum number of missed cleavages equal to two; precursor mass tolerance equal to 20 ppm; fragment mass tolerance equal to 20 ppm; variable modifications, dimethly Lys (light, +28.0313 D), dimethy N-term (light, +28.0313 D), dimethly Lys (heavy, +34.0631 D), dimethy N-term (heavy, +34.0631 D). The data were filtered

by applying a 1% false discovery rate followed by exclusion of proteins with fewer than two unique peptides. Quantified proteins were filtered if the absolute fold change difference between the three replicates was ≥1.3.

Section B3. Cellular functional analysis of PS-ApTCs.

Cell viability assay of PS-ApTCs. Cell viability assay was performed by using Cell Counting Kit-8 (CCK-8). Briefly, HeLa cells or L-02 cells were seeded in 96-well plates (about 10^4 cells per well), followed by treating with 200 μL of 200 nM PS-ApTCs, R-PROTACs or PS-AS1411 for given time points (0 h, 3 h, 6 h, 9 h, 12 h and 24 h) at 37℃, respectively. Then, the cells were washed three times with DPBS buffer and subsequently incubated with 10 μL of the CCK-8 reagent into each well for 30 min. Absorption at 450 nm was measured using a microplate reader (Bio-Tek Instrument, Winooski, VT, USA).

For the dose-dependent cell viability experiments, HeLa cells were treated with different concentrations (0.2-400 nM) of PS-ApTCs, R-PROTACs, or PS-AS1411 for 48 h at 37℃, and the cell viability were then analyzed following the same protocol as above.

Analysis of cell apoptosis after PS-ApTCs treatment. The effect of PS-ApTCs on cell apoptosis was measured by Annexin V and PI staining followed by flow cytometry. Briefly, HeLa cells or L-02 cells were were first cultured in 6-well plates, and grown until it reached 70-80% confluency. After that, the cells were washed three times with DPBS buffer, and subsequently treated with 1000 μL of 200 nM PS-ApTCs, R-PROTACs or PS-AS1411 for 48 h, respectively. Then, the resulting cells were washed with DPBS buffer, and subsequently digested with with 0.25% trypsin (1.0 mL) for 10 min at 37℃. After that, the cell apoptosis assays were performed using an Annexin V-FITC Apoptosis kit (556547, BD Pharmingen™, USA) according to the manufacturer's instruction, and analyzed at ~200 cells/sec on a Beckman Coulter CytoFLEX flow cytometry system (Beckman Coulter Inc., USA). Untreated cells were used as the control. The percentages of cells in early and late apoptosis were quantified with FlowJo software.

Analysis of cell cycle after PS-ApTCs treatment. The effect of PS-ApTCs on cell cycle was also performed using flow cytometry with a similar procedure in Section B3, except for the replacement of the Annexin V-FITC Apoptosis kit with a Cell Cycle Detection kit.

Section B4. Cellular functional analysis of synergistically designed PS-ApTCs/ApDCs.

Design and mass characterization of GSH-responsive ApDCs. The GSH-responsive ApDCs was synthesized using a similar procedure in Section B1, except for the replacement of the DBCO-AS1411-PS and pomalidomide-PEG4-azide with DBCO-AS1411-intSH and PTX-PEG_{1000}-azide, respectively. The obtained ApDCs was characterized using MALDI-TOF mass spectrometry, which was recorded on an ABI-MDS SCIEX 4800 Plus MALDI TOF/TOF™ mass spectrometer.

***In vitro* cleavage assay.** *In vitro* cleavage assay was performed to assess the GSH-responsive property of DBCO-AS1411-intSH. Briefly, 2 μL of 10 μM DBCO-AS1411-intSH was first mixed with 2 μL of 20 mM GSH and 16 μL of Millipore water. After incubation for 1 h at 37℃, the mixture solution was immediately analyzed by 15% native polyacrylamide gel electrophoresis (nPAGE) with the following experimental conditions: voltage (80 V), 0.5X TBE buffer, 80 min.

In addition, the HPLC-based cleavage assay was similar to a previously described procedure in Section B4, except for the replacement of 10 μM DBCO-AS1411-intSH with 10 μM ApDCs. The resulting solutions were carried out on Thermo Scientific Dionex Ultimate 3000 with CH_3CN/H_2O (100 mM Ammonium acetate)

as the eluents for the HPLC assay. For comparison, untreated ApDCs, fragment 1, and fragment 2 were applied as controls and analyzed following the same protocol as above.

Immunoblots analysis of cytoplasmic nucleolin degradation by PS-ApTCs/ApDCs. The effect of PS-ApTCs/ApDCs on the cytoplasmic nucleolin levels was analyzed following the same protocol in Section B2, except for the replacement of 200 nM PS-ApTCs with 200 nM of ApTCs/ApDCs. For comparison, untreated HeLa cells or cells treated with 200 nM of PS-ApTCs or ApDCs were applied as controls.

Cell viability, apoptosis, and cell cycle analysis of PS-ApTCs/ApDCs. The effects of PS-ApTCs/ApDCs on cell viability, apoptosis, and cell cycle were performed by following the same protocol in Section B3, except for the replacement of 200 nM PS-ApTCs with 200 nM of ApTCs/ApDCs. For comparison, untreated HeLa cells or cells treated with 200 nM of PS-ApTCs or ApDCs were applied as controls.

Drug synergy of PS-ApTCs and Control-PS-ApTCs. Drug synergy was evaluated using the Bliss independence model.[4] Briefly, the predicted fractional growth inhibition of the drug combination is calculated using the equation $f_1 + f_2 - (f_1 \times f_2)$, where f_1 and f_2 are the fractional growth inhibitions of the individual drugs 1 and 2 at a given dose. Bliss excess is the difference between the expected growth inhibition and the observed inhibition from the drug combination. The Bliss score was normalized in a way that values less than 0 represent antagonism, close to 0 represent additivity, and values larger than 0 represent synergy. Bliss sum is the sum of individual Bliss scores of drug doses.

The synergy effects of PS-ApTCs/ApDCs on cell viability were performed by following the same protocol in Section B3. For comparison, HeLa cells treated with different concentration of Control-PS-ApTCs and ApDCs were applied as control group.

Quantitative reverse transcription-PCR (qRT-PCR) assay of p53 gene. The effect of PS-ApTCs/ApDCs on the mRNA levels of p53 in HeLa cells was evaluated by quantitative qRT-PCR. Briefly, HeLa cells were first treated with 200 nM of PS-ApTCs, ApDCs, or PS-ApTCs/ApDCs for 48 h at 37°C, respectively. Then, the resulting cells were lysed, and total RNA was extracted using Total RNA Isolation Kit (Shanghai Sangon Biotech, B511321) according to the manufacturer's instruction. RNA concentration was determined spectroscopically using the Nanodrop (Thermo Scientific), and 1 μg of total RNA was reverse transcribed using PrimeScriptTM RT reagent Kit (RR047A, TaKaRa, China). The resulting cDNA samples were further amplified using real-time PCR with the primers indicated in Table S1 and a TB Green® Premix Ex Taq™ (RR420A, TaKaRa, China). All qRT-PCR were performed on a LightCycler® 96 System (Roche), and all results were quantified using the comparative threshold cycle (Cq) method. The mRNA level of β-actin was used as the internal control to normalize Cq values of each reaction.

Section B5. In vivo synergistic therapy using PS-ApTCs/ApDCs.

Ethical statement and animal model. Animal husbandry and the experimental protocols used in this study were approved by the Institutional Animal Care and Use Committee (IACUC) of Nanjing University (animal protocol number: IACUC-2204009). The experiments also comply with the 'Animal Research: Reporting *In Vivo* Experiments' (ARRIVE) 2.0 guidelines (https://arriveguidelines.org/arrive-guidelines). The BALB/c nude mice were purchased from the Changzhou Cavens Laboratory Animal Ltd,. The HeLa cervical cancer xenograft model was established by subcutaneous injection of HeLa cells (100 μL, 1×10^6) into the right hind leg of female BALB/c nude mice (5-6 weeks old). When the tumor size reached ~100 mm^3, fluorescence imaging and therapeutic experiments were performed.

***In vivo* imaging.** The BALB/c nude mice bearing HeLa cervical cancer xenograft model were intravenously injected with 50 μL of 50 μM Cy5, R-PROTACs-Cy5 and PS-ApTCs-Cy5, respectively. Then the nude mice were anesthetized and imaged with a IVIS Lumina XR III *in vivo* imaging system (PerkinElmer, USA). In addition, the tumors and major organs (including heart, liver, kidney and lung) were also collected at 8 h post-injection and subjected to ex vivo fluorescence imaging with the aforementioned IVIS imaging system.

Design of ligation-PCR strategy for PS-ApTCs screening. The ligase-assisted PCR (ligation-PCR) system contains two key components: (1) the PS-ApTCs as the template to assists the ligation by hybridization with two ligation primers at the ligation region; (2) The ligation products were analyzed by quantitative PCR (qPCR) to quantify PS-ApTCs.

In a typical ligation-PCR experiment, 2.0 μL of PS-ApTCs was pre-incubated with 2.0 μL of 10X T4 DNA ligase buffer, 2.0 μL of Ligation primer 1 (10 nM), 2.0 μL of Ligation primer 2 (10 nM), 2.0 μL of T4 DNA ligase (40 units/μL), and 10 μL Millipore water at 16°C for 20 min to enable ligation reaction. After heat inactivation at 75°C for 10 min, the ligation products were amplified and analyzed by a qPCR using a TB Green® Premix Ex Taq reagent Kit (RR420A, TaKaRa), in which TB Green was utilized as the fluorescent dye for real-time detection of the PCR products.

All qPCRs were performed on a LightCycler® 96 System (Roche). The PCR reaction mixture contains 2 μL of above ligation products, 0.4 μL of forward primer (10 μM), 0.4 μL of reverse primer (10 μM), 7 μL Millipore water, and 10 μL of 2X PCR mix from the qPCR Kit. The PCR reaction mixture was subjected to qPCR according to the following thermal cycle: 45 cycles of 95 °C for 10 s, 65 °C for 60 s. The qPCR curves and Ct values were analyzed using LightCycler® 96 Application Software (Roche).

For PS-ApTCs detection in mouse whole blood, 1.0 μL of different concentrations of PS-ApTCs was prepared in 100% mouse whole blood, and tested according to the typical ligation-PCR experiment.

Pharmacokinetics Study. The pharmacokinetics studies were performed in BALB/c nude mice (n = 3) bearing HeLa cervical cancer xenograft model. The mice were kept overnight in a fasting condition with the free access of water throughout the experiment. PS-ApTCs were administered to mice through the intravenous injection at a dose of 300 nmol/kg. After a complete dosage (taken as zero time), a volume of 30 μL of whole blood was collected into EDTA-K2 anticoagulant tubes at time points 10 min, 2, 4, 6, 8, 12, and 24 h. Then, 30 mL of DPBS were added to each sample and vortexed for 15 s. Finally, the samples were purified by Amicon-30K and detected by ligation-PCR assay.

All pharmacokinetic analyses were made using classical techniques and the microcomputer-based program Phoenix WinNonlin 5.2.1 software (Pharsight Corp., St. Louis, MO, USA).

To enable detection *in vivo*, 5.85 nmol of Cy5-PS-ApTCs was administered by tail vein injection and tracked with a IVIS Lumina XR III *in vivo* imaging system (PerkinElmer, USA). The time points were set at 10 min, 0.5, 1, 2, 4, 6, 8, 10,12, and 24 h, respectively. Fluorescence was analyzed with IVIS Living Imaging 3.0 software.

***In vivo* therapy.** The BALB/c nude mice bearing HeLa cervical cancer xenograft model were randomly divided into four groups (four mice per group) when the average tumor volume reached to about 100 mm^3. Then, the mice were intravenously injected with PBS (control group), or 5.85 nmol of PS-ApTCs, ApDCs, and PS-ApTCs/ApDCs every three days, respectively. The tumor growth and body weight were monitored every other day. The length and width of each tumor were recorded, and the tumor volumes were calculated with the following formula: Volume=(length × $width^2$)/2. The tumor growth inhibition (TGI) were calculated using the following formula: TGI = [1-(ΔT/ΔC)] × 100% (ΔT = mean tumor volume changes in the drug treatment group

and ΔC = mean tumor volume changes in the control group). All animal procedures were in accord with the guidelines of the Institutional Animal Care and Use Committee.

Histology. After 19 days post-treatment, the mice were sacrificed, and the tumors and major organs (including heart, liver, spleen, kidney and lung) were separated for hematoxylin-eosin (H&E) staining, immunohistochemical analysis, Ki67 immunofluorescence analysis and terminal deoxynucleotidyl transferase-mediated dUTP nick-end labeling (TUNEL) assays. Histology examination was performed with assistance from the Servicebio Biotech Company (Wuhan, China).

***In vivo* nucleolin protein expressions.** Western blot analysis were used to assess the cytoplasmic NCL protein levels in tumors. Typically, after 19 days post-treatment, the mice were sacrificed, and tumors were separated for the extraction of cytoplasmic proteins. Subsequently, the protein expression was evaluated following the similar procedures as mentioned in the *in vitro* experiments following the same protocol in Section B2.

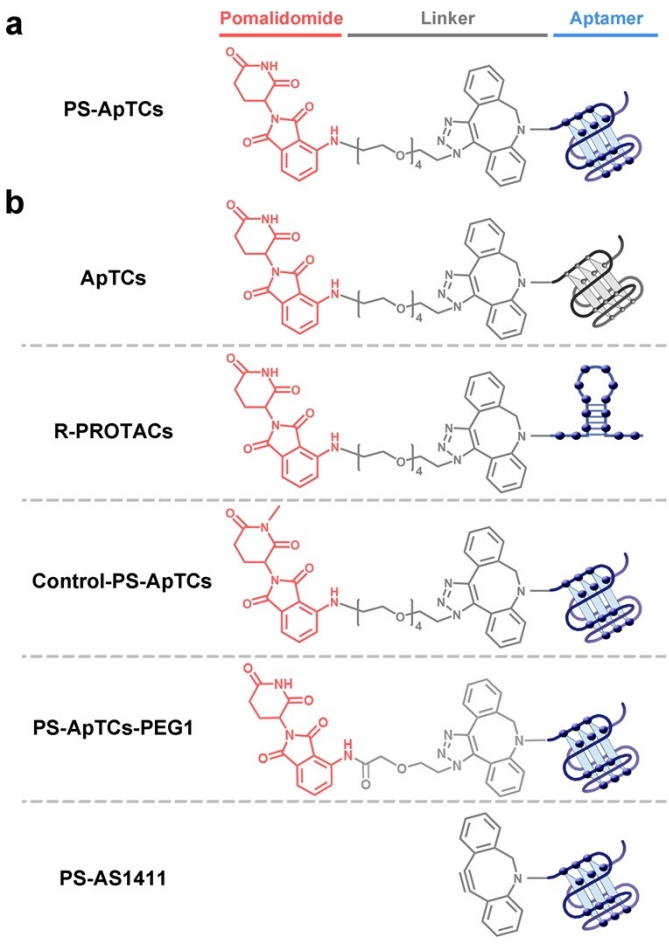

Fig. S1. Rational design of (a) phosphorothioate-modified Aptamer-PROTACs (PS-ApTCs), (b) Aptamer-PROTACs (ApTCs), randomized DNA sequence-based PROTAC (R-PROTAC), N-methyl glutarimide analog (Control-PS-ApTCs), PS-ApTCs with 1-polyethylene glycols (PEGs) linker (PS-ApTCs-PEG1), and PS-AS1411.

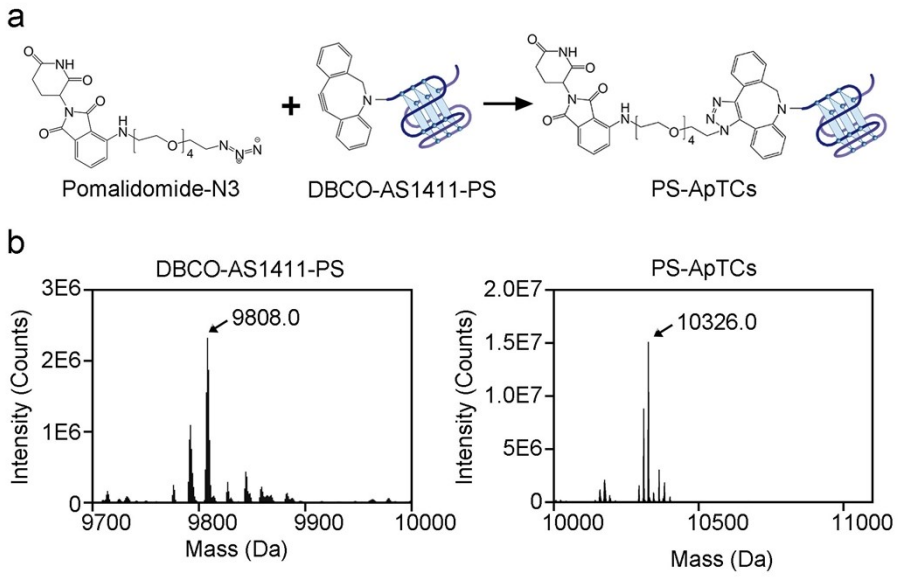

Fig. S2. (a) Synthetic strategy of PS-ApTCs. (b) Mass analysis of DBCO-AS1411-PS and PS-ApTCs. DBCO-AS1411-PS: calculated molecular weight: 9808.9, Found: 9808.0; PS-ApTCs: calculated molecular weight: 10326.9, Found: 10326.0.

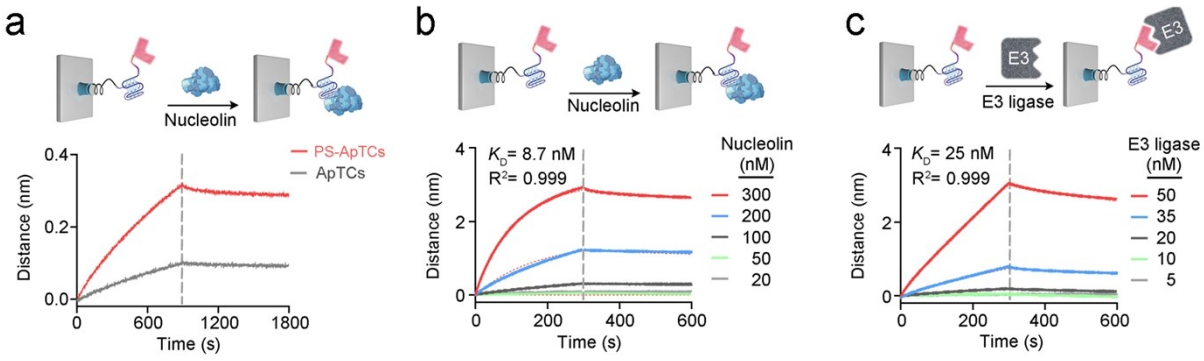

Fig. S3. (a) BLI experiment showing PS-ApTCs displays higher binding affinity to NCL than ApTCs. Quantitative BLI analysis showing that PS-ApTCs binds to NCL and CRBN with a K_D of 8.7 nM (b) and 25 nM (c), respectively. Solid lines represent the response curves of BLI measurement, and dotted lines represent the fitting curves based on the 1:1 monovalent binding model.

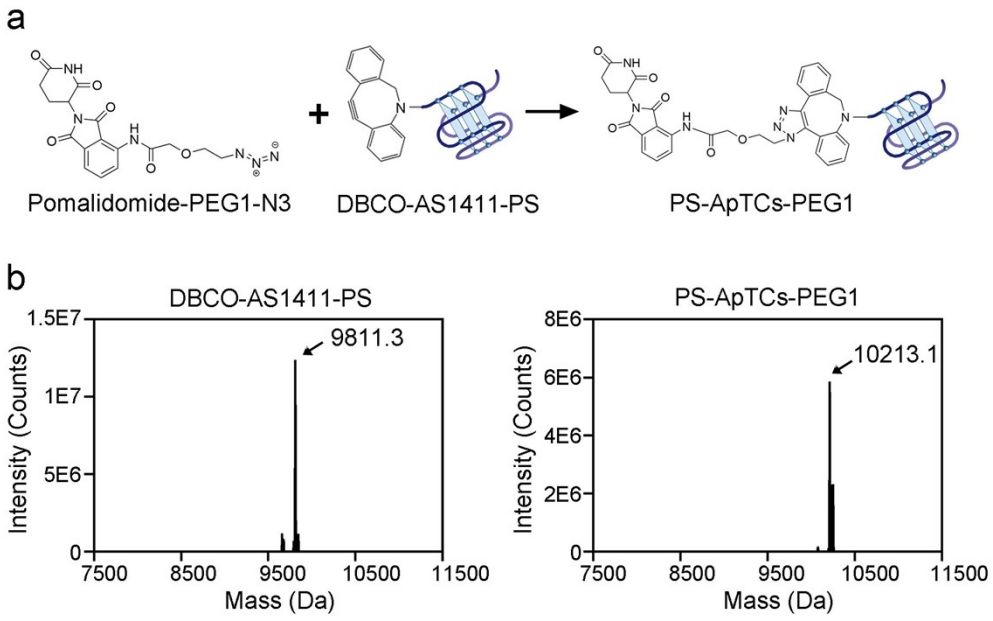

Fig. S4. (a) Synthetic strategy of PS-ApTCs-PEG1. (b) Mass analysis of DBCO-AS1411-PS and PS-ApTCs by Sangon (Shanghai). DBCO-AS1411-PS: calculated molecular weight: 9808.9, Found: 9811.3; PS-ApTCs-PEG1: calculated molecular weight: 10209.3, Found: 10213.1. Mass analysis was performed on a Thermo LTQ Orbitrap XL mass spectrometer. The source voltage was set at 4500 V with a heated capillary temperature of 350°C.

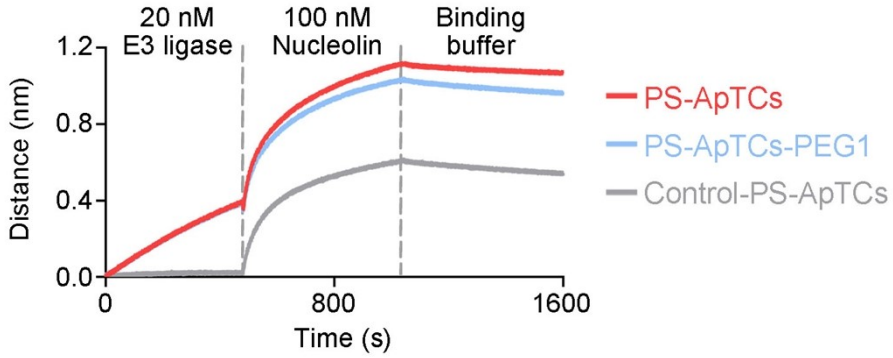

Fig. S5. Two-step BLI characterization of PS-ApTCs, PS-ApTCs-PEG1, and Control-PS-ApTCs. Biotin-modified PROTACs were captured by streptavidin BLI probes. Ternary complex formation between CRBN, NCL and PROTACs was investigated by successive incubating the Biotin-modified PROTACs (100 nM) immobilized BLI sensor in 20 nM CRBN and 100 nM NCL solutions.

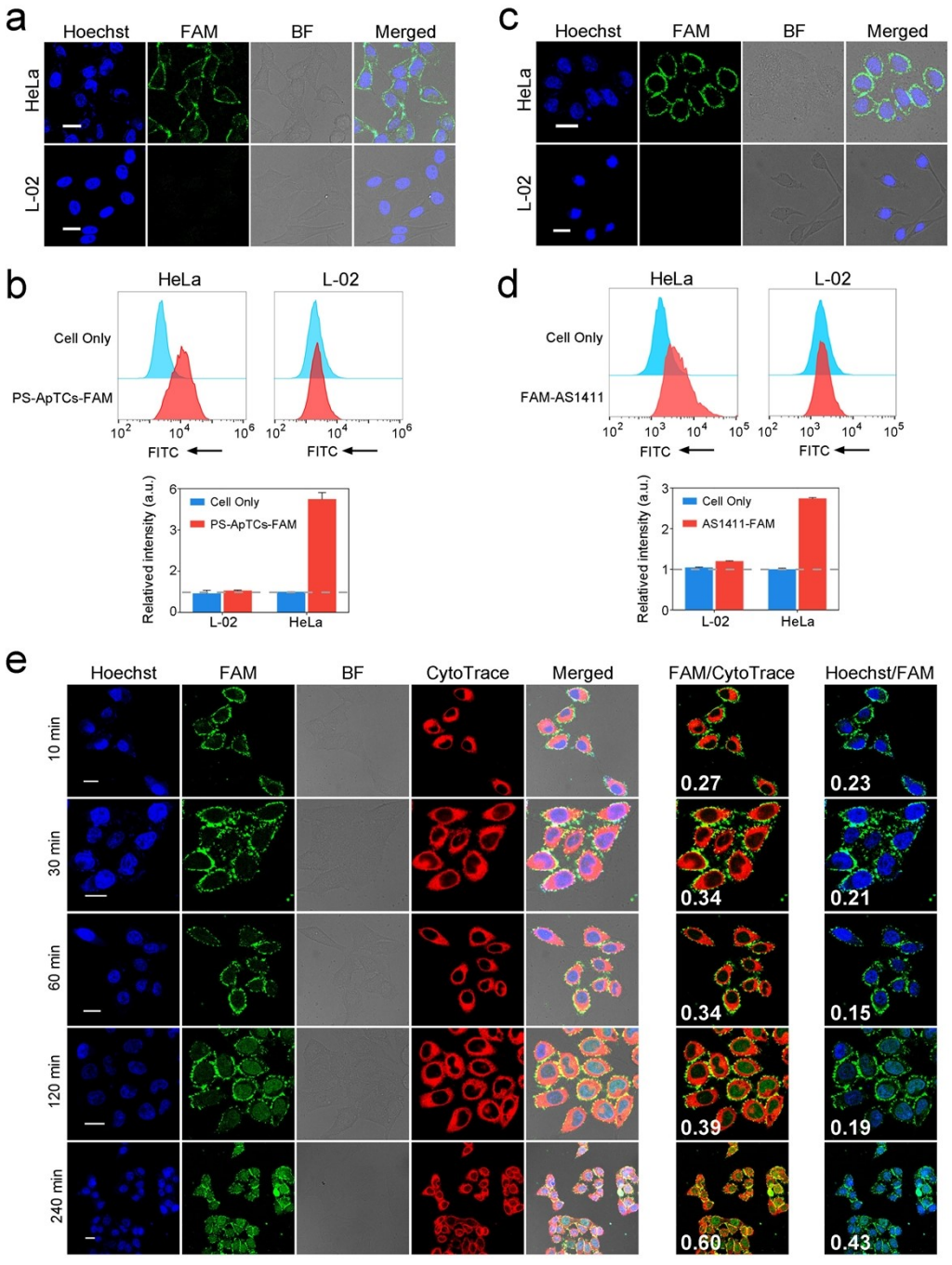

Fig. S6. PS-ApTCs selectively binds to cervical cancer cells. Confocal laser scanning micrographs for HeLa cells and L-02 cells after incubation with 200 nM PS-ApTCs-FAM (a) and FAM-AS1411 (c) for 1 h at 4°C. The binding of PS-ApTCs-FAM (b) and FAM-AS1411 (d) to HeLa and L-02 cells was analyzed by flow cytometry. Error bars represent the standard deviations of three independent measurements. (e) Confocal microscopy imaging of HeLa cells incubated with PS-ApTCs-FAM at different time points, the MOC quantifying the degree of colocalization of the two fluorescence signals. The green and red colors represent PS-ApTCs-FAM and CytoTrace red, respectively. Scale bar: 20 μm.

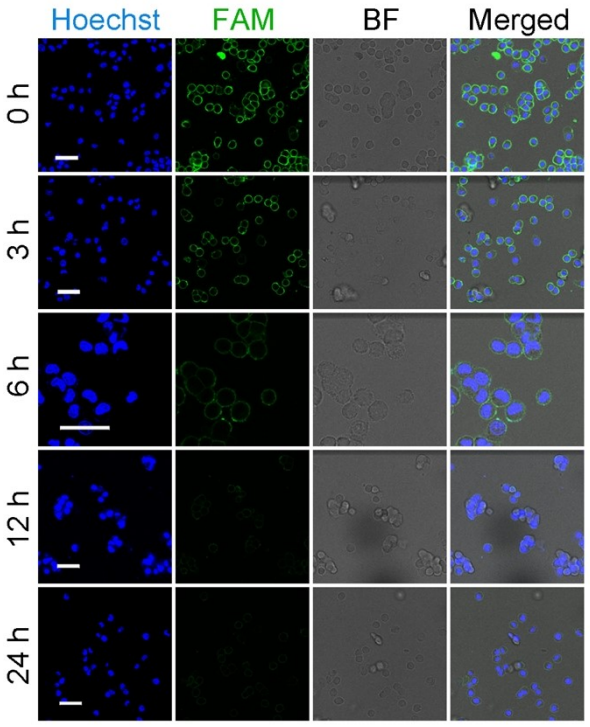

Fig. S7. Confocal microscopy images showing a time-dependent decrease of membrane NCL levels in HeLa cells post-incubation with 200 nM PS-ApTCs in the wide field of view. Membrane NCL was labeled with FAM-AS1411 (green) at 4℃ for 60 min. The scale bar is 40 μm.

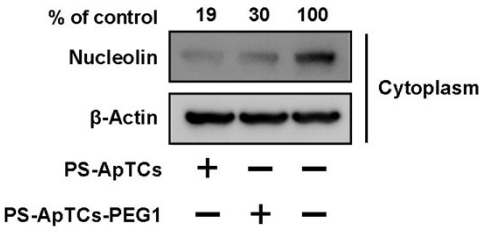

Fig. S8. Immunoblots analysis of cytoplasmic NCL protein levels in HeLa cells treated with 200 nM PS-ApTCs and PS-ApTCs-PEG1 for 24 hours. The symbols "+" and "-", indicate the presence and absence of the corresponding molecules, respectively. Compared with PBS-treated group, both PS-ApTCs and PS-ApTCs-PEG1 resulted in an efficient degradation of cytoplasmic NCL, while the former showed a relatively enhanced NCL degradation.

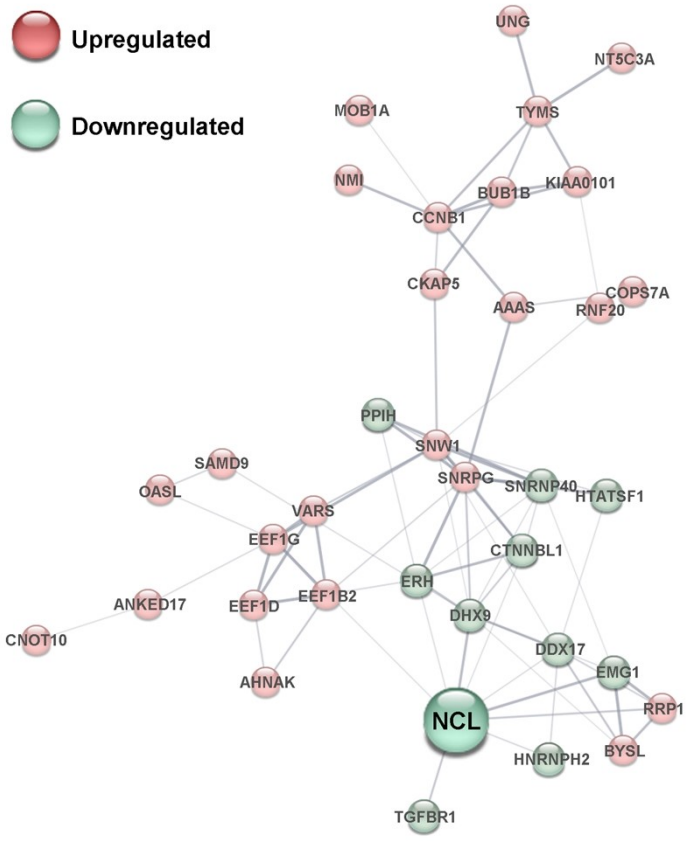

Fig. S9. STRING network involving NCL and the proteins that were up- and down-regulated in HeLa cells treated with PS-ApTCs compared to PS-AS1411-treated cells. (STRING: https://string-db.org/).

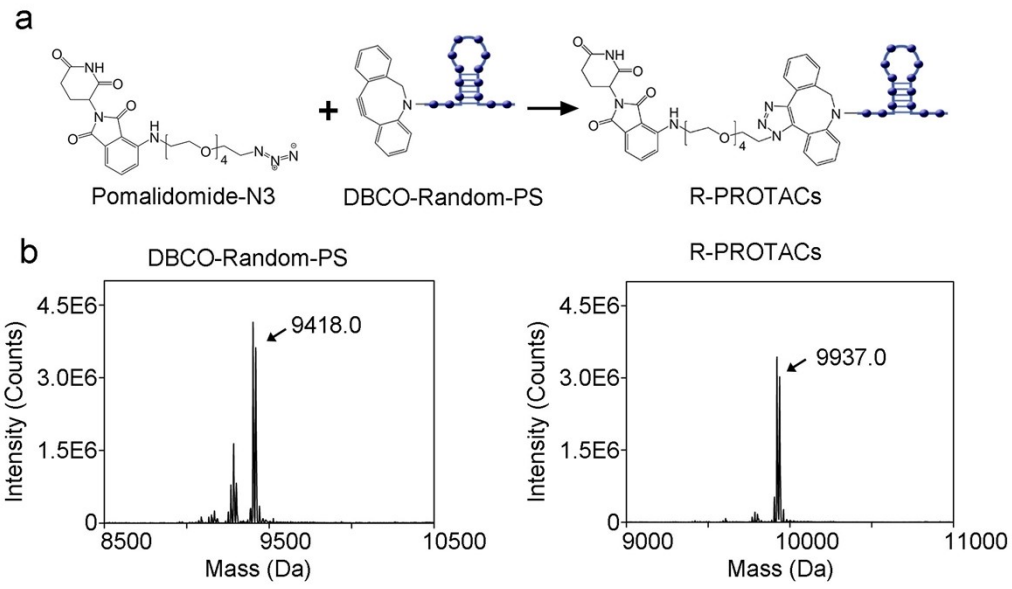

Fig. S10. (a) Synthetic strategy of R-PROTACs. (b) Mass analysis of DBCO-Random-PS and R-PROTACs. DBCO-Random-PS: calculated molecular weight: 9419.7, Found: 9418.0; R-PROTACs: calculated molecular weight: 9937.7, Found: 9937.0.

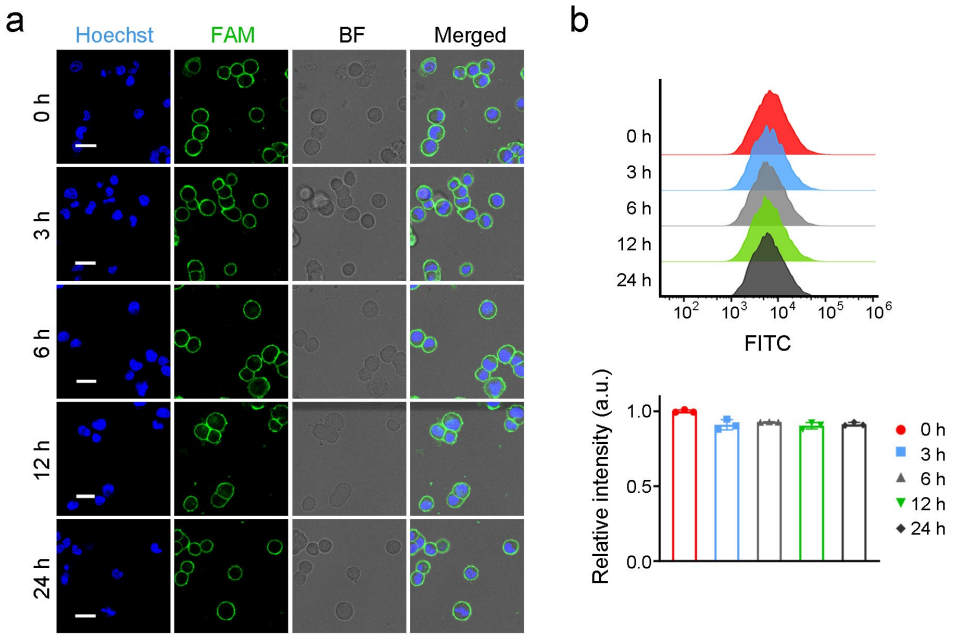

Fig. S11. (a) Fluorescence imaging of nucleolin levels in HeLa cell membranes post-incubation with R-PROTACs using confocal fluorescence microscopy. HeLa cells were incubated with 200 nM R-PROTACs for 0 h (No treatment), 3 h, 6 h, 12 h or 24 h in cell culture medium at 37°C, followed by labeling nucleolin receptor with FAM-AS1411 aptamer (green) at 4°C for 60 min. (b) Flow cytometry analysis of nucleolin levels in HeLa cell membranes post-incubation with 200 nM R-PROTACs. Error bars represent the standard deviations of three independent measurements. The scale bar is 20 μm.

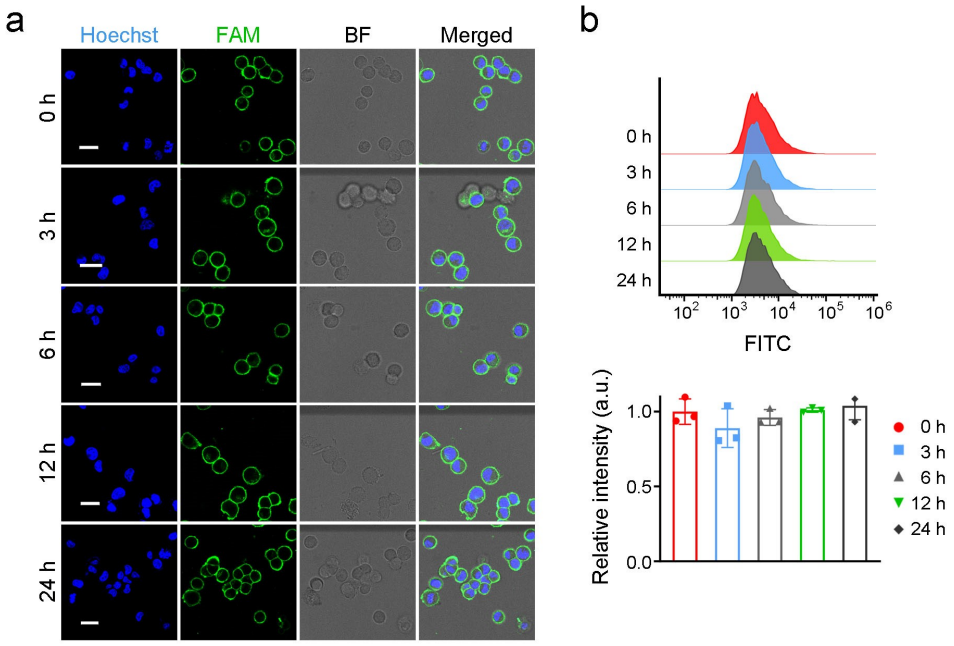

Fig. S12. (a) Fluorescence imaging of nucleolin levels in HeLa cell membranes post-incubation with PS-AS1411 using confocal fluorescence microscopy. HeLa cells were incubated with 200 nM PS-AS1411 for 0 h (No treatment), 3 h, 6 h, 12 h or 24 h in cell culture medium at 37℃, followed by labeling nucleolin receptor with FAM-AS1411 aptamer (green) at 4°C for 60 min. (b) Flow cytometry analysis of nucleolin levels in HeLa cell membranes post-incubation with 200 nM PS-AS1411. Error bars represent the standard deviations of three independent measurements. The scale bar is 20 μm.

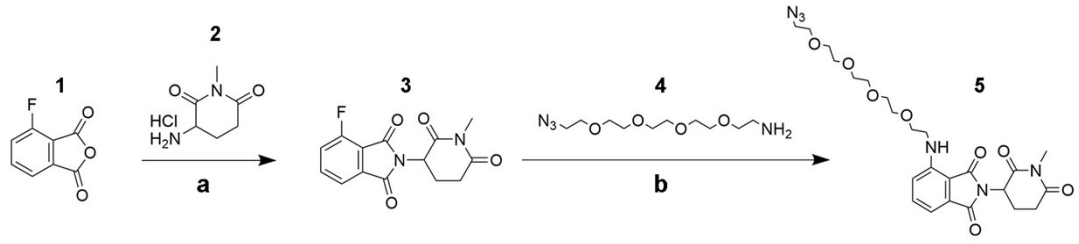

Fig. S13. Synthetic strategy of azide-modified N-methyl pomalidomide. a) NaOAc, AcOH, 63%; b) DIPEA, DMF, 32%.

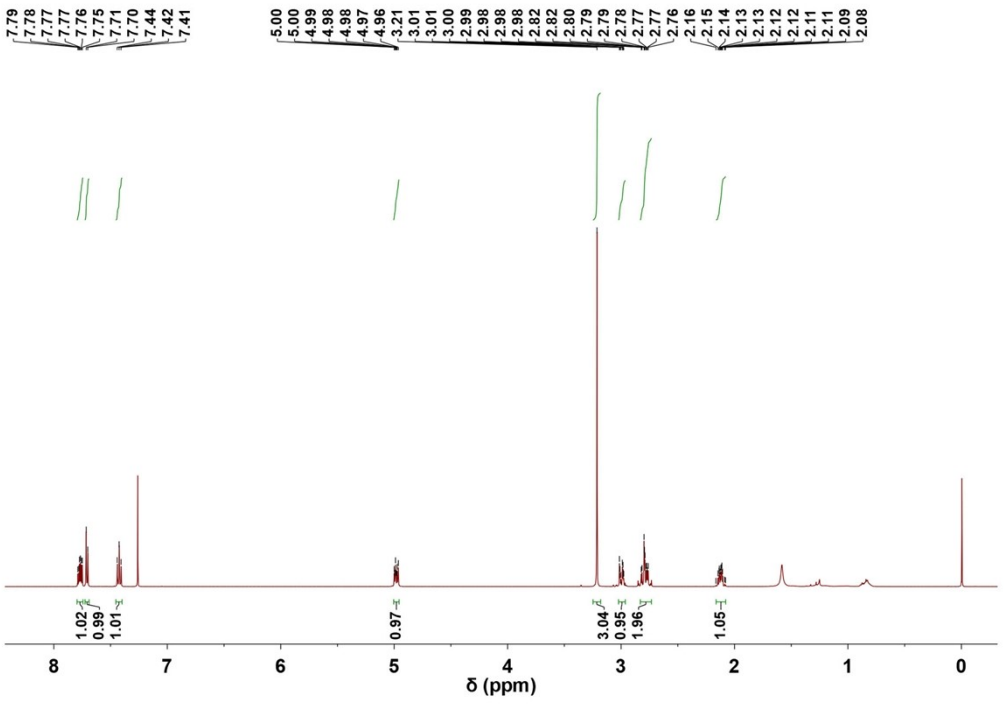

Fig. S14. ^{1}H NMR spectra of 4-Fluoro-2-(1-methyl-2,6-dioxo-3-piperidyl)isoindoline-1,3-dione (compound 3). ^{1}H NMR (500 MHz, $CDCl_3$): δ 7.79 - 7.76 (m, 1H), 7.71 (d, *J* = 6.5 Hz, 1H), 7.42 (t, *J* = 8.5 Hz, 1H), 5.00 - 4.96 (m, 1H), 3.21 (s, 3H), 3.01 - 2.98 (m, 1H), 2.82 - 2.76 (m, 2H), 2.16 - 2.08 (m, 1H).

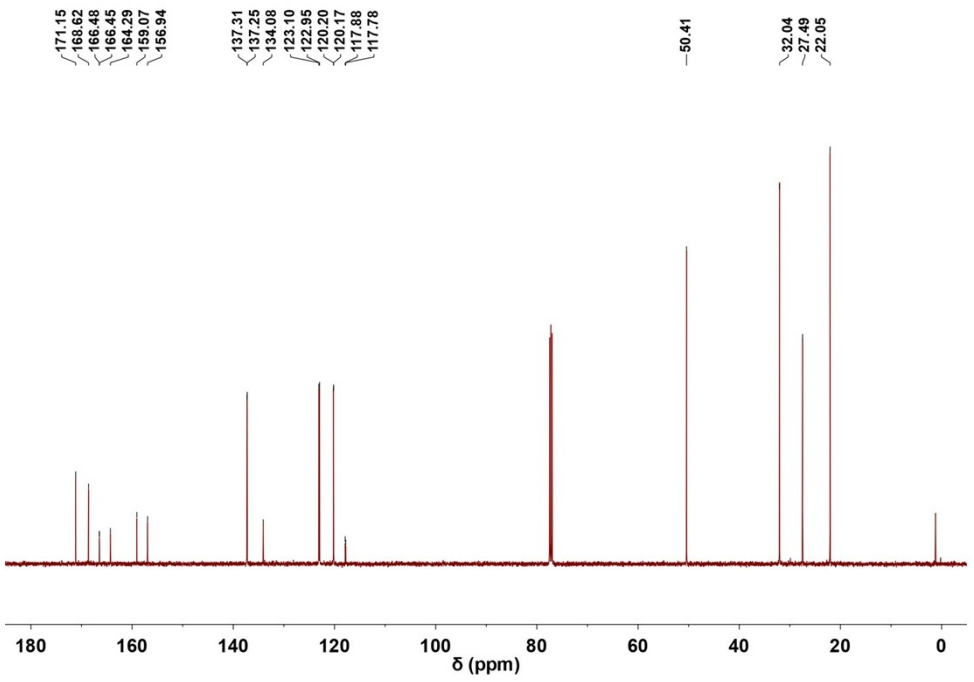

Fig. S15. ^{13}C NMR spectra of 4-Fluoro-2-(1-methyl-2,6-dioxo-3-piperidyl)isoindoline-1,3-dione (compound 3). ^{13}C NMR (126 MHz, $CDCl_3$): δ 22.05, 27.49, 32.40, 50.41, 117.83 (d, ^{2}J (C, F) = 12.6 Hz), 123.02 (d, ^{2}J (C, F) = 19.8 Hz), 120.18 (d, ^{4}J (C, F) = 3.7 Hz), 134.08, 137.28 (d, ^{3}J (C, F) = 7.9 Hz), 158.01 (d, ^{1}J (C, F) = 267.4 Hz), 164.29, 166.46 (d, ^{3}J (C, F) = 2.9 Hz), 168.62, 171.15.

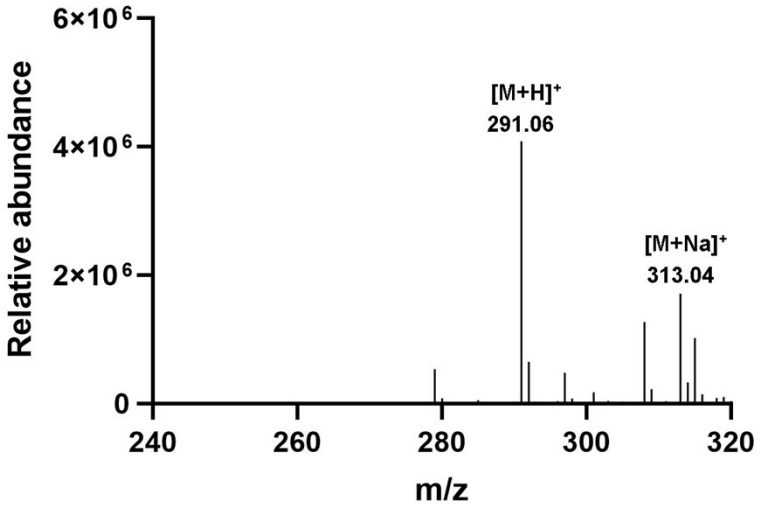

Fig. S16. Positive mode mass spectra of 4-Fluoro-2-(1-methyl-2,6-dioxo-3-piperidyl)isoindoline-1,3-dione (compound 3). $C_{14}H_{12}FN_2O_4$ $[M+H]^+$ calcd. m/z 291.08; found 291.06; $[M+Na]^+$ calcd. m/z 313.06; found 313.04.

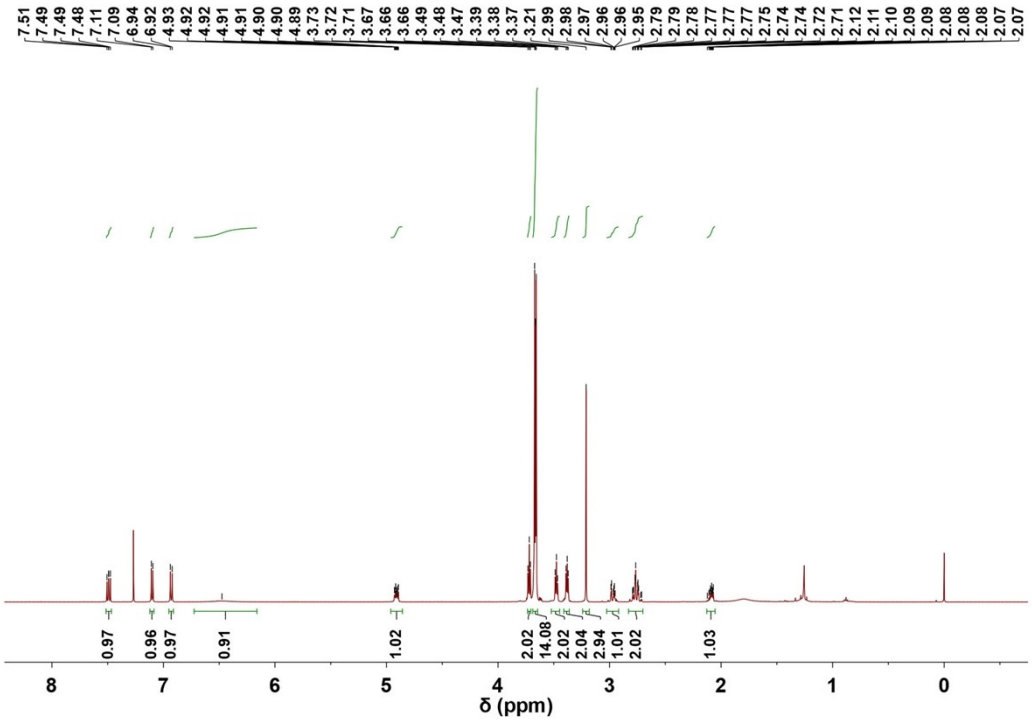

Fig. S17. ^{1}H NMR spectra of 4-((14-azido-3,6,9,12-tetraoxatetradecyl)amino)-2-(1-methyl-2,6-dioxopiperidin-3-yl)isoindoline-1,3-dione (compound 5). δ 7.49 (dd, J = 8.5, 7.1 Hz, 1H), 7.10 (d, J = 7.1 Hz, 1H), 6.93 (d, J = 8.4 Hz, 1H), 6.48 (br s, 1H), 4.93 - 4.89 (m, 1H), 3.72 (t, J = 5.6 Hz, 2H), 3.67 - 3.66 (m, 14H), 3.48 (t, J = 5.5 Hz, 2H), 3.38 (t, J = 5.3 Hz, 2H), 3.21 (s, 3H), 2.99 - 2.95 (m, 1H), 2.79 - 2.71 (m, 2H), 2.12 - 2.07 (m, 1H).

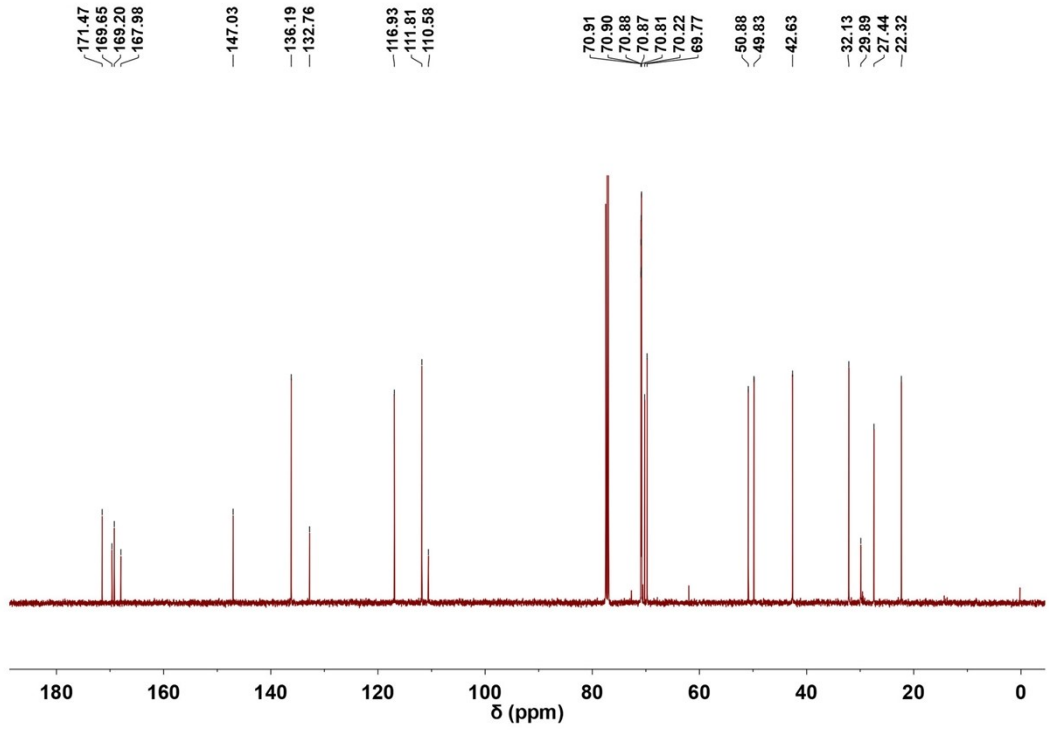

Fig. S18. ^{13}C NMR spectra of 4-((14-azido-3,6,9,12-tetraoxatetradecyl)amino)-2-(1-methyl-2,6-dioxopiperidin-3-yl)isoindoline-1,3-dione (compound 5). ^{13}C NMR (126 MHz, $CDCl_3$): δ 22.32 (C-4'), 27.44 (NCH_3), 29.89 (C-5'), 32.13 ($NHCH_2$), 42.63 (CH_2N_3), 49.83 (C-3'), 50.88, 70.91, 70.90, 70.88, 70.87, 70.81, 70.22, 69.77 (OCH2), 110.58 (C-3a), 111.81 (C-7), 116.93 (C-5), 132.76 (C-7a), 136.19 (C-6), 147.03 (C-4), 167.98 (C-1), 169.20 (C-3), 169.65 (C-2'), 171.47 (C-6').

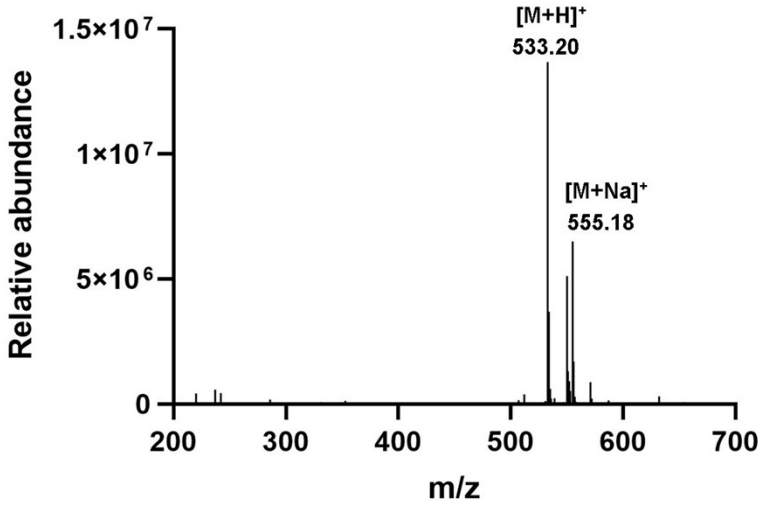

Fig. S19. Positive mode mass spectra of 4-((14-azido-3,6,9,12-tetraoxatetradecyl)amino)-2-(1-methyl-2,6-dioxopiperidin-3-yl)isoindoline-1,3-dione (compound 5). $C_{24}H_{32}N_6O_8$ $[M+H]^+$ calcd. m/z 533.23; found 533.20; $[M+Na]^+$ calcd. m/z 555.21; found 555.18.

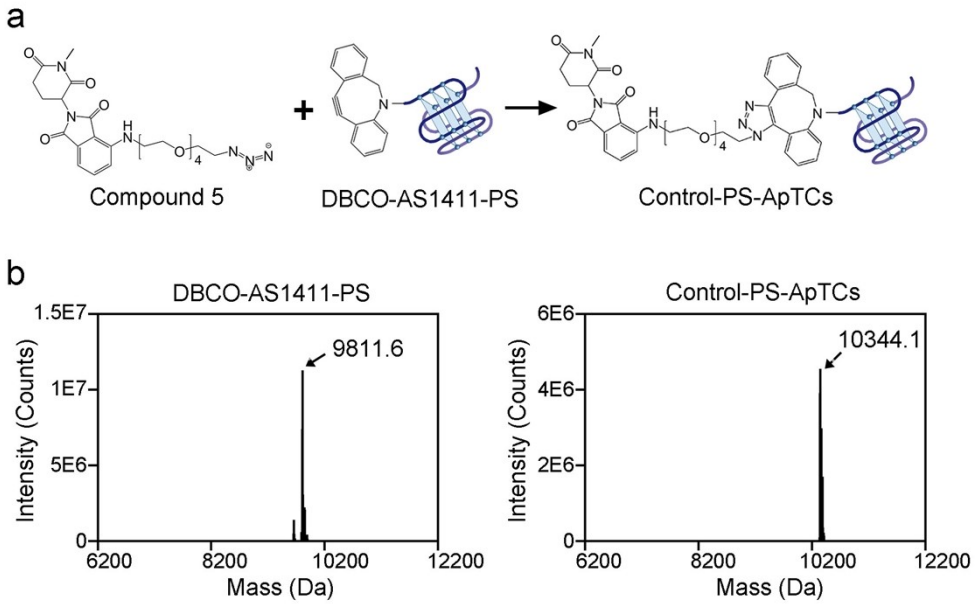

Fig. S20. (a) Synthetic strategy of Control-PS-ApTCs. (b) Mass analysis of DBCO-AS1411-PS and Control-PS-ApTCs by Sangon (Shanghai). DBCO-AS1411-PS: calculated molecular weight: 9808.9, Found: 9811.6; Control-PS-ApTCs: calculated molecular weight: 10341.1, Found: 10344.1. Mass analysis was performed on a Thermo LTQ Orbitrap XL mass spectrometer. The source voltage was set at 4500 V with a heated capillary temperature of 350°C.

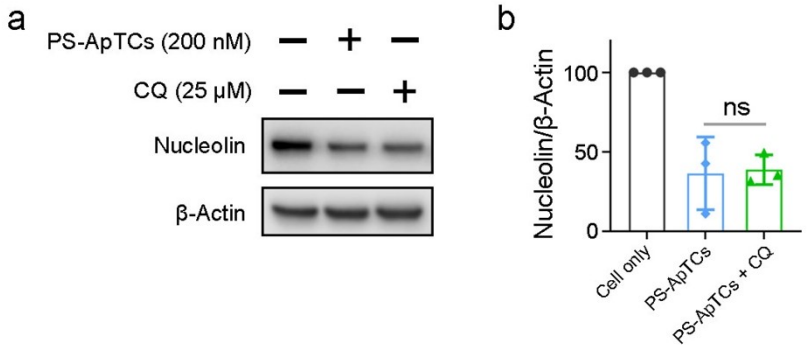

Fig. S21. (a) Effect of lysosome inhibitor CQ on cytoplasmic NCL degradation in HeLa cells after treating with PS-ApTCs (200 nM) and CQ (25 μM) for 24 h. (b) Quantitative analysis of the cytoplasmic NCL from the assays presented in (a). ns: no significant difference.

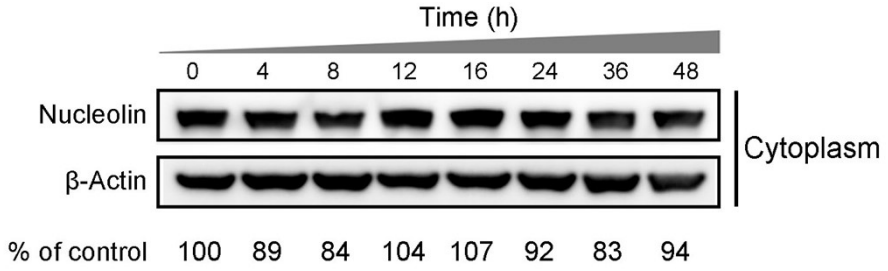

Fig. S22. Western blot analysis of cytoplasmic NCL protein levels in L-02 cells treated with 200 nM PS-ApTCs for different time points.

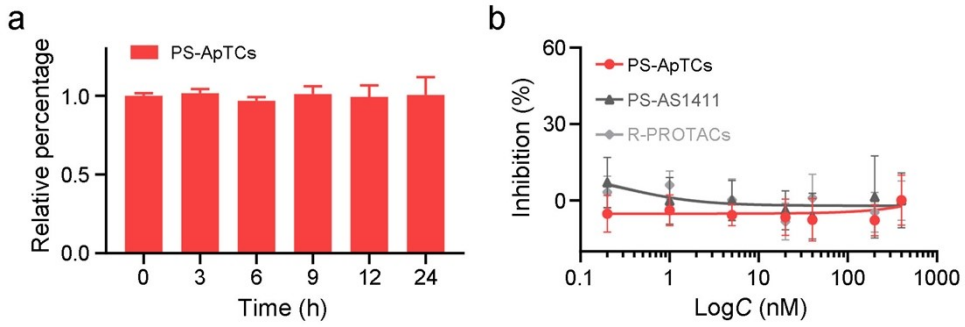

Fig. S23. (a) Cell viability of L-02 cells treated with 200 nM of different PROTACs as indicated for different times in cell culture medium at 37℃. (b) Cell viability of L-02 cells treated with different concentrations of PROTACs as indicated in cell culture medium for 48 h at 37℃. Error bars represent the standard deviations of three independent measurements.

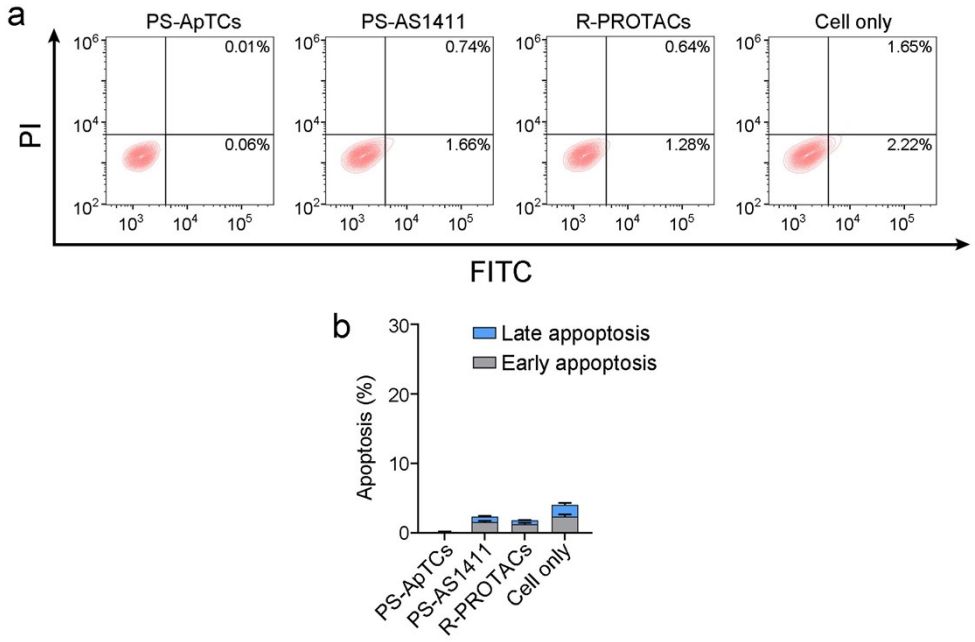

Fig. S24. (a) Flow cytometry analysis of L-02 cells post-incubation with 200 nM of different PROTACs for 48 h, followed by staining with Annexin V-FITC and propidium iodide. (b) Quantitative analysis of the levels of early- and late-stage apoptosis from the assays presented in (a). Error bars represent the standard deviations of three independent measurements.

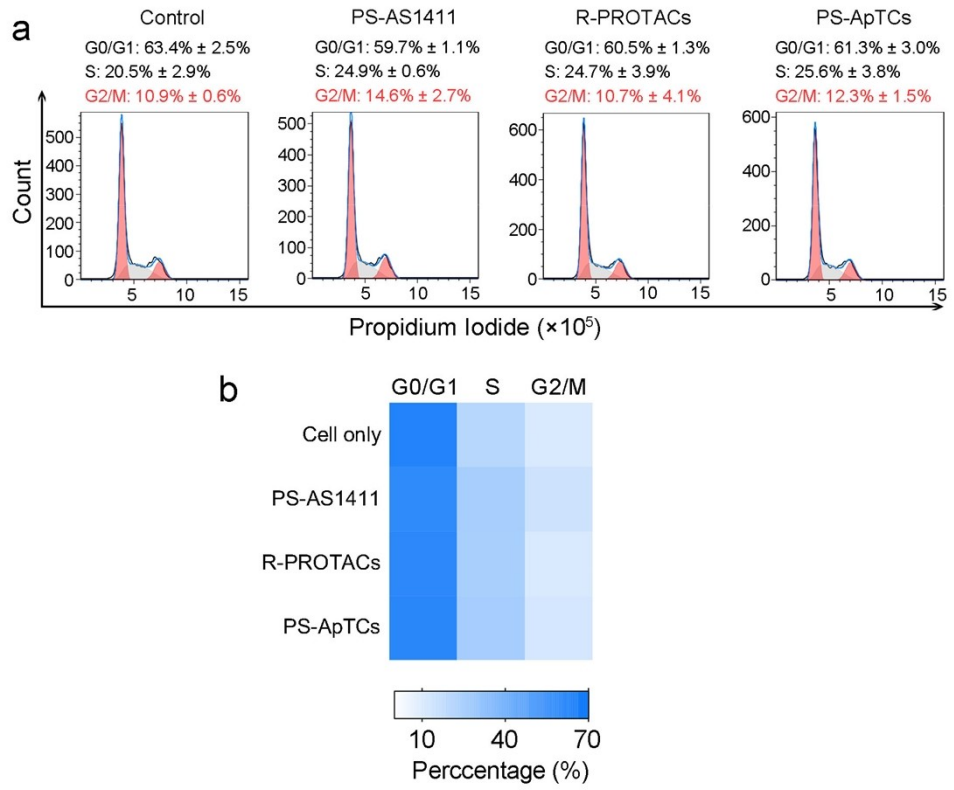

Fig. S25. (a) Cell cycle analysis of L-02 cells treated with 200 nM of different PROTACs, as determined by flow cytometry using propidium iodide staining. Histograms from a representative experiment showing G0/G1 and G2/M populations shaded in red and S phase population in gray. The vertical and the horizontal axes represent cell number and fluorescence intensity, respectively. (b) Representative heatmaps of cell cycle distribution from the assays presented in (a).

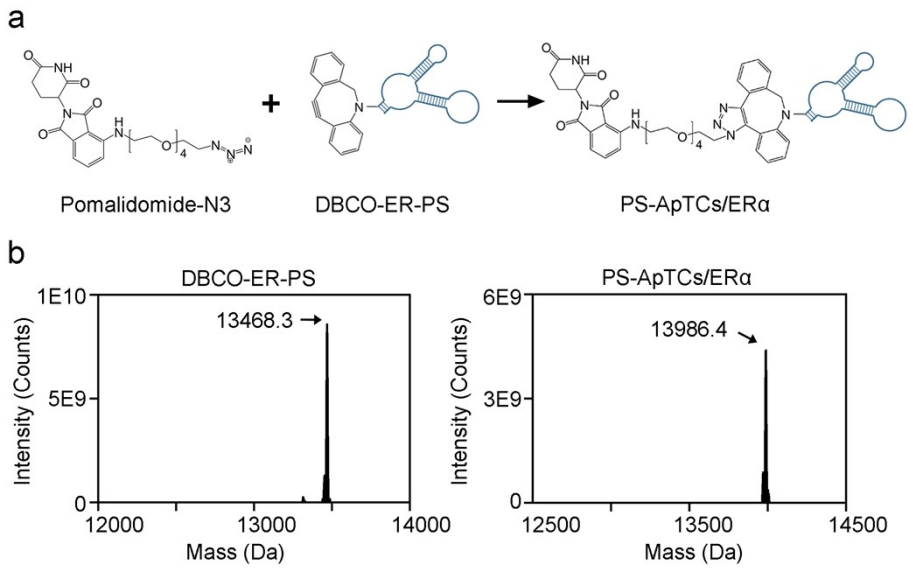

Fig. S26. (a) Synthetic strategy of PS-ApTCs/ERα. (b) Mass analysis of DBCO-ER-PS and PS-ApTCs/ERα. DBCO-ER-PS: calculated molecular weight: 13466.9, Found: 13468.3; PS-ApTCs/ERα: calculated molecular weight: 13984.9, Found: 13986.4.

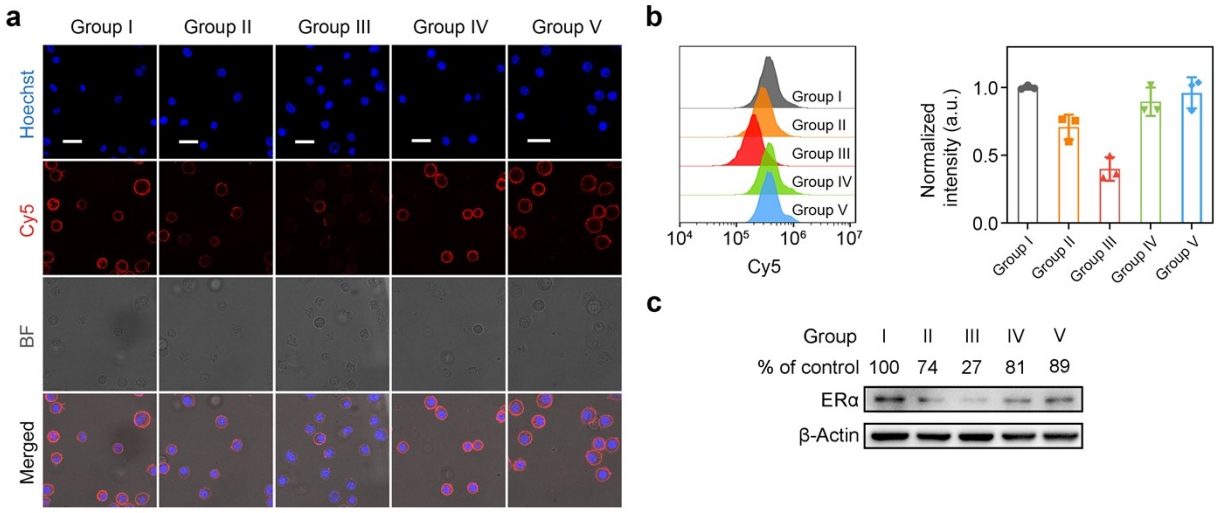

Fig. S27. PS-ApTCs/ERα efficiently degraded membrane and cytoplasmic ERα in MCF-7 cells. Confocal microscopy images (a) and flow cytometry analysis (b) demonstrate that PS-ApTCs/ERα can degrade membrane ERα protein levels in MCF-7 cells. The scale bar is 30 μm. MCF-7 cells were first incubated with various drug groups for 24 h, and then stained with Cy5-ERα/apt at 4°C to assess the degradation of ERα on the cell membrane. (c) Western blot analysis of cytoplasmic ERα levels after treatment with various drug groups. Group I: MCF-7 cells; Group II: MCF-7 cells + 400 nM PS-ApTCs/ERα; Group III: MCF-7 cells + 2000 nM PS-ApTCs/ERα; Group IV: MCF-7 cells + 200 nM MG132 + 2000 nM PS-ApTCs/ERα; Group V: MCF-7 cells + 100 nM MLN4924 + 2000 nM PS-ApTCs/ERα.

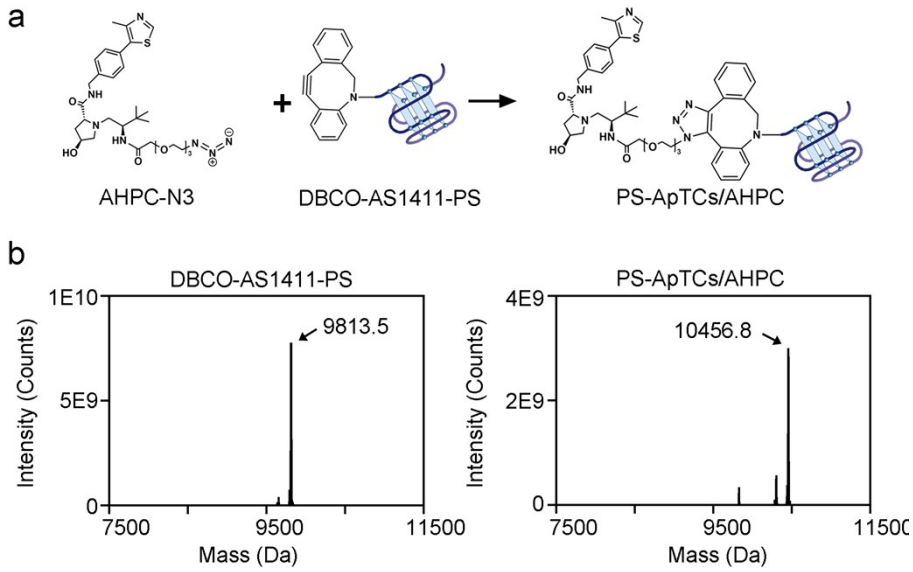

Fig. S28. (a) Synthetic strategy of PS-ApTCs/AHPC. (b) Mass analysis of DBCO-AS1411-PS and PS-ApTCs/AHPC. DBCO-AS1411-PS: calculated molecular weight: 9808.9, Found: 9813.5; PS-ApTCs/AHPC: calculated molecular weight: 10454.7, Found: 10456.8.

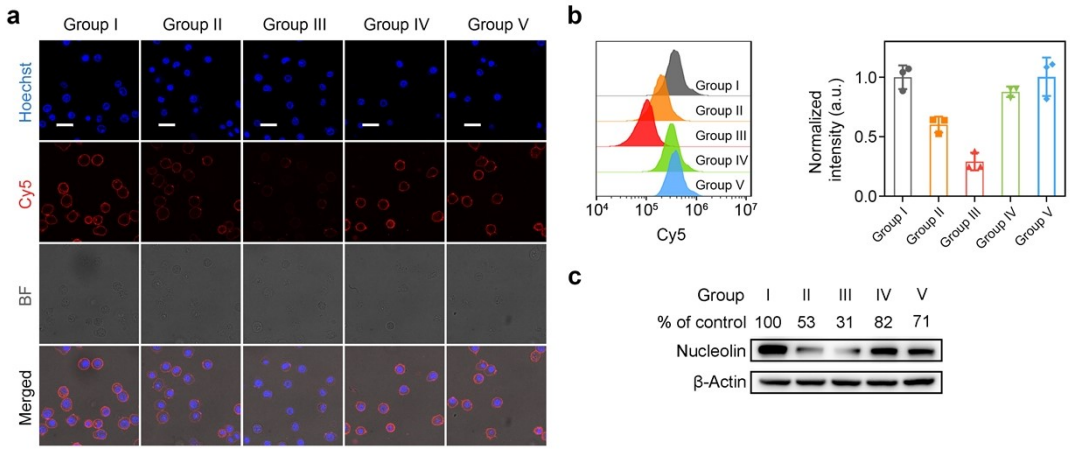

Fig. S29. PS-ApTCs/AHPC efficiently degraded membrane and cytoplasmic NCL in HeLa cells. Confocal microscopy images (a) and flow cytometry analysis (b) demonstrate that PS-ApTCs/AHPC can degrade membrane NCL levels in HeLa cells. The scale bar is 30 μm. HeLa cells were first incubated with various drug groups for 24 h, and then stained with Cy5-AS1411 at 4°C to assess the degradation of NCL on the cell membrane. (c) Western blot analysis of cytoplasmic NCL levels after treatment with various drug groups. Group I: HeLa cells; Group II: HeLa cells + 40 nM PS-ApTCs/AHPC; Group III: HeLa cells + 200 nM PS-ApTCs/AHPC; Group IV: HeLa cells + 200 nM MG132 + 200 nM PS-ApTCs/AHPC; Group V: HeLa cells + 100 nM MLN4924 + 200 nM PS-ApTCs/AHPC.

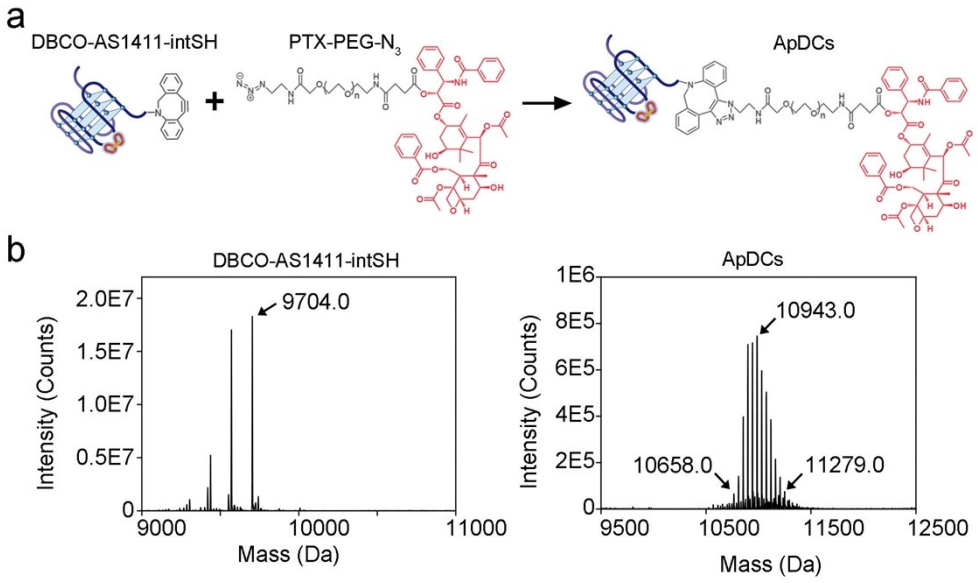

Fig. S30. (a) Synthetic strategy of ApDCs. (b) Mass analysis of DBCO-AS1411-intSH and ApDCs. DBCO-AS1411-intSH: calculated MW of 9703.7, found MW of 9704; ApDCs: calculated MW of 10900~11500, found MW of 10658~11279.

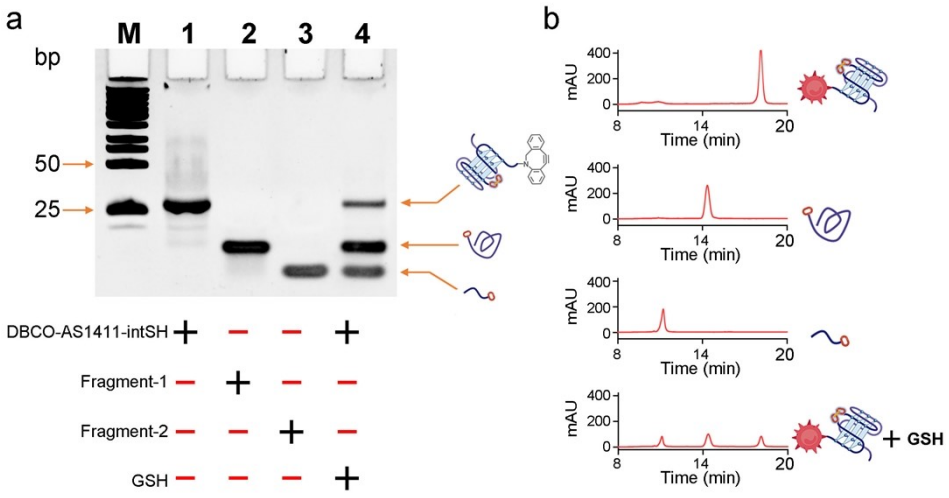

Fig. S31. The nPAGE (a) and HPLC (b) assay verified that ApDCs can be cleaved by GSH. Low MW DNA ladder with a MW range of 25−766 bp (New England Biolabs, China) was used as the size marker. The symbols "+" and "-", indicate the presence and absence of the corresponding molecules, respectively.

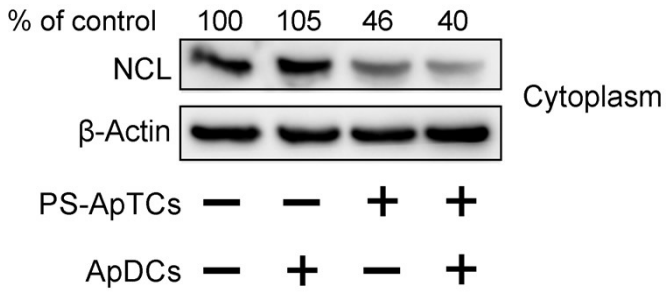

Fig. S32. Immunoblots analysis to validate the feasibility of the PS-ApTCs/ApDCs for nucleolin degradation in cytoplasm. The symbols "+" and "-", indicate the presence and absence of the corresponding molecules, respectively.

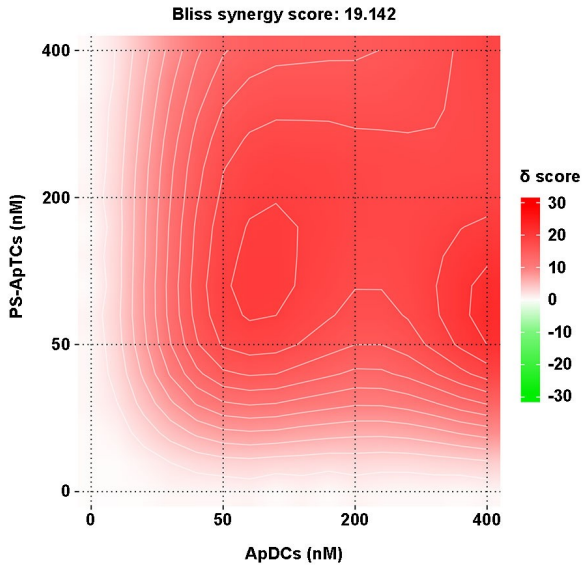

Fig. S33. Synergy matrix plot showing δ-scores for HeLa cells were treated with PS-ApTCs and ApDCs alone and in combination at the indicated concentrations for 24 h. Synergy maps were generated using the SynergyFinder web application (https://synergyfinder.fimm.fi).

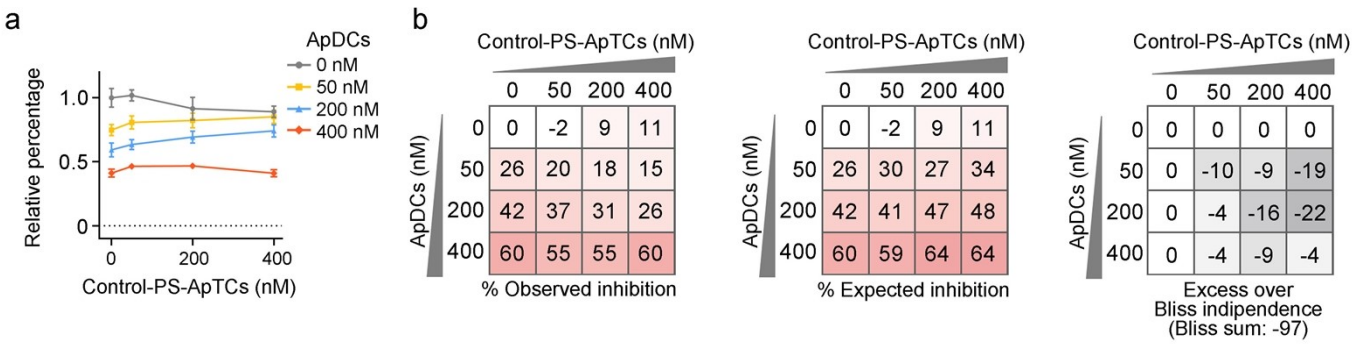

Fig. S34. Drug synergy test of Control-PS-ApTCs and ApDCs using Bliss independence model. (a) HeLa cells were treated with Control-PS-ApTCs and ApDCs alone and in combination at the indicated concentrations for 24 h. (b) Drug synergy represented by excess over Bliss scores were calculated based on the Bliss Independence model at each combination of drug doses.

a

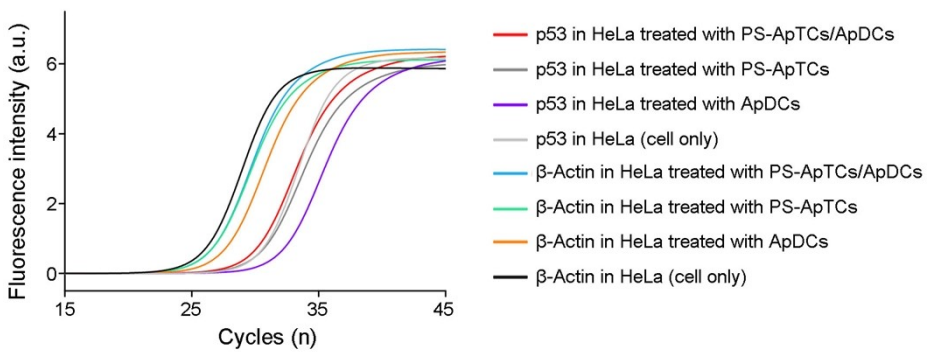

b

HeLa treated with	p53	β-Actin	△Cq	△△Cq	$2^{-(\triangle\triangle Cq)}$
PS-ApTCs/ApDCs	28.27	24.75	3.52	-1.36	2.57
PS-ApTCs	28.90	24.58	4.32	-0.56	1.47
ApDCs	30.05	25.78	4.27	-0.61	1.53
Cell only	29.15	24.27	4.88	0	1

Fig. S35. (a) Quantitative reverse transcription-PCR curves for p53 and β-Actin mRNA extracted from PS-ApTCs/ApDCs-treated HeLa cells, PS-ApTCs-treated HeLa cells, ApDCs-treated HeLa cells and untreated HeLa cells. (b) Average Cq value in qRT-PCR assay of p53 estimated from $2^{-(\Delta\Delta Cq)}$. Error bars represent the standard deviations of three independent measurements.

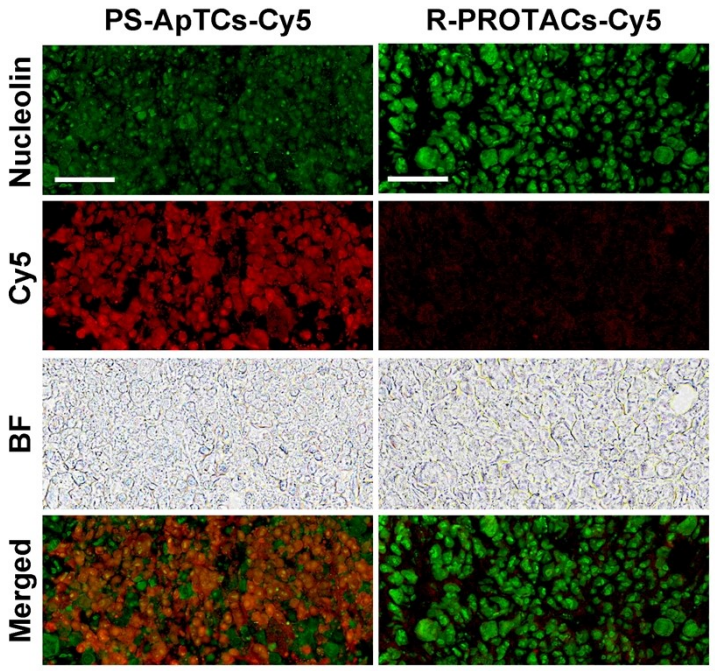

Fig. S36. The representative fluorescent micrographs of the frozen tissue sections from tumors treated with PS-ApTCs-Cy5 or R-PROTACs-Cy5. Immunofluorescence staining was performed 8 h after intravenous injection using Alexa488-labeled anti-nucleolin antibody (green). Scale bars = 50 μm.

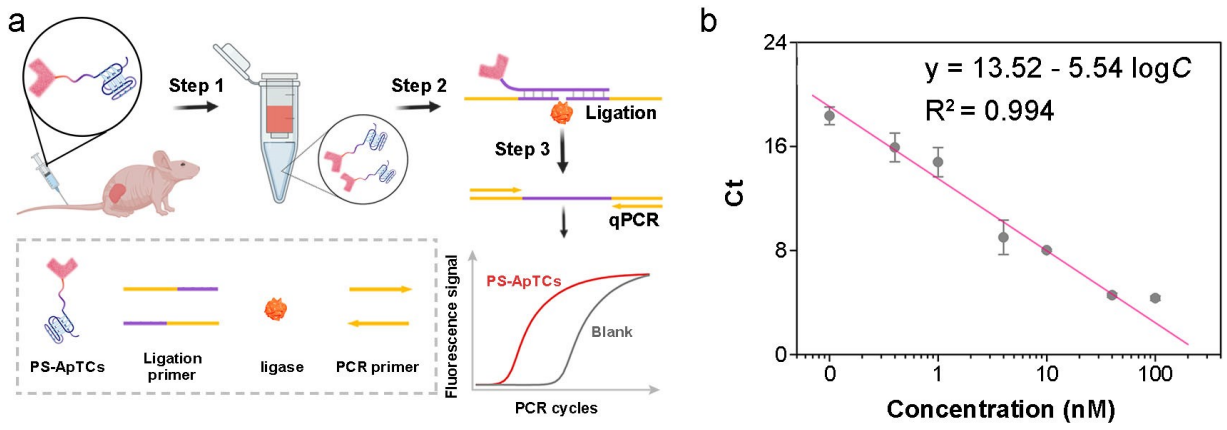

Fig. S37. (a) Detection strategy and workflow of ligation-qPCR assay for PS-ApTCs screening. (Bb) Linear relationship of PCR Ct value and PS-ApTCs concentrations.

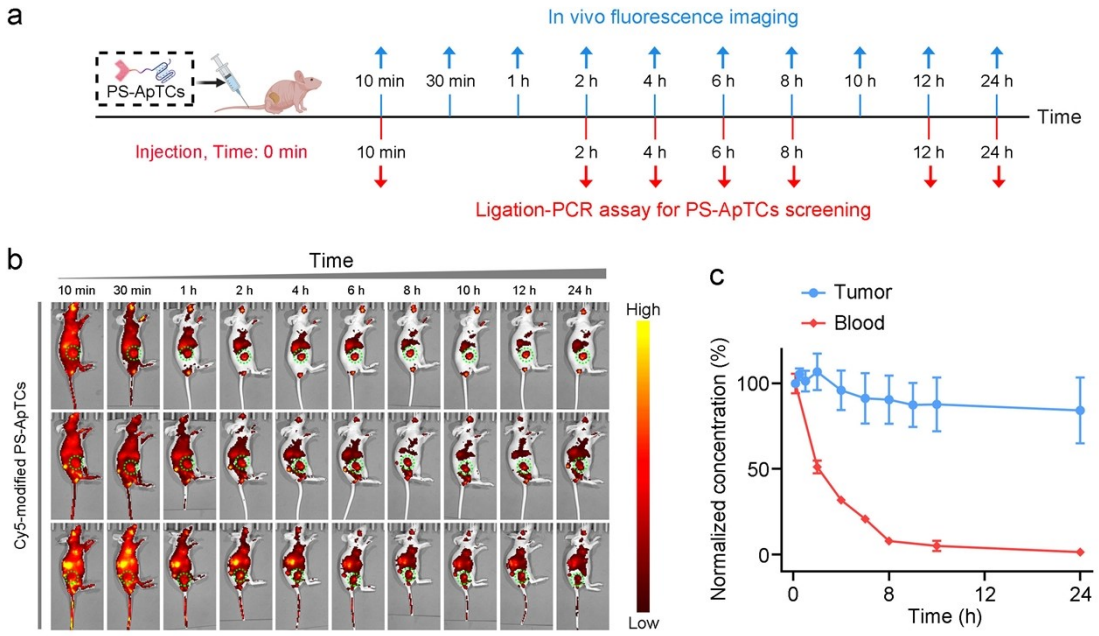

Fig. S38. (a) Schematic displaying the pharmacokinetic assay in the mouse model. The points of fluorescence imaging and ligation-PCR assay are indicated with blue and red arrows, respectively. (b) *In vivo* fluorescence whole body imaging to evaluate the distribution of PS-ApTCs-Cy5 in HeLa xenograft mouse ($n = 3$) at different time points after single tail vein injection (300 nmol/kg). (c) Quantitative biodistribution analysis of PS-ApTCs-Cy5 in blood and tumors.

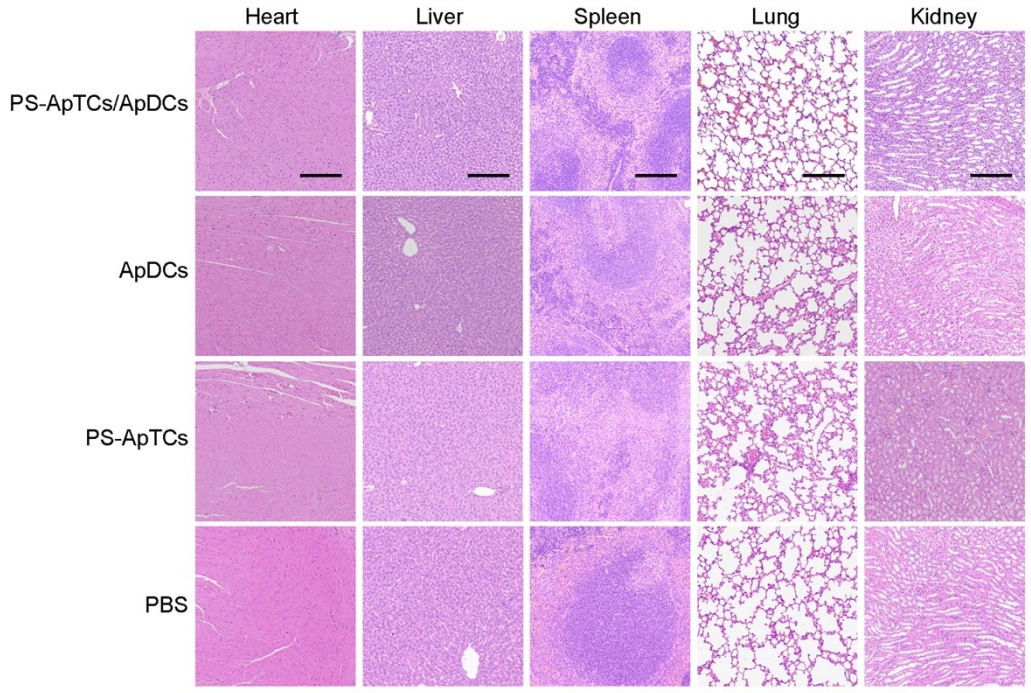

Fig. S39. Microphotographs of H&E stained major organs after different treatments. Scale bars=200 μm.

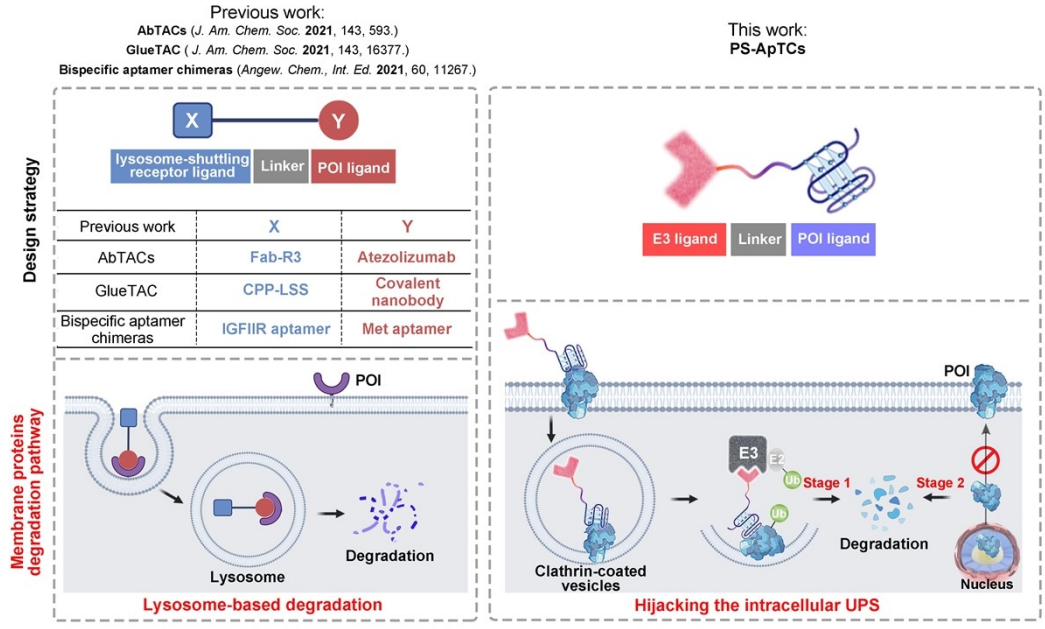

Fig. S40. Comparision of previous degradation mechanism for membrane protein with our PS-ApTCs.

Table S1. Sequences of DNA oligonucleotides used in this work[a]

Name	Sequence (5'-3')
DBCO-modified AS1411 (DBCO-AS1411)	DBCO-TTGGTGGTGGTGGTTGTGGTGGTGGTGG
Phosphorothioate-modified DBCO-AS1411 (PS-AS1411)	DBCO-T*T*G*G*T*G*G*T*G*G*T*G*G*T*T*G*T*G*G*T*G*G*T*G*G*T*G*T*G*G
Biotin-modified DBCO-AS1411 (DBCO-AS1411-Biotin)	DBCO-TTGGTGGTGGTGGTTGTGGTGGTGGTGG-Biotin
Biotin-modified DBCO-AS1411-PS (DBCO-AS1411-PS-Biotin)	DBCO-T*T*G*G*T*G*G*T*G*G*T*G*G*T*T*G*T*G*G*T*G*G*T*G*G*T*G*T*G*G-Biotin
FAM-modified AS1411 (FAM-AS1411)	FAM-TTGGTGGTGGTGGTTGTGGTGGTGGTGG
Cy5-modified AS1411 (Cy5-AS1411)	Cy5-TTGGTGGTGGTGGTTGTGGTGGTGGTGG
Phosphorothioate-modified DBCO-ERα(DBCO-ERα-PS)	DBCO-C*C*C*G*G*C*A*T*G*G*T*T*G*C*G*G*A*G*C*A*G*G*A*G*T*A*T*A*A*C*A*C*T*A*C*C*A*T*T*G
Cy5-modified ERα aptamer (Cy5-ERα)	Cy5-CCCGGCATGGTTGCGGAGCAGGAGTATAACACTACCATTG
DBCO and phosphorothioate-modified Random aptamer (DBCO-Random-PS)	DBCO-T*T*A*C*T*T*G*C*A*T*T*A*C*C*G*T*A*A*C*A*C*A*T*G*C*A*C*A
DBCO and thiol-modified (DBCO-AS1411-intSH)	DBCO-TTGGTGGTGG/int SH-SH/TGGTTGTGGTGGTGGTGG
Fragment 1	TGGTTGTGGTGGTGGTGG
Fragment 2	TTGGTGGTGG
Ligation primer 1	TTGCTCAGTCACTTCTTTGTCGTCTTCATGACCCACCACCA
Ligation primer 2	P-CCACAACCACCACCACCAAGTATTATCCTAGTTCCTAGACACGACCAA
Forward primer (PS-ApTCs)	TTGCTCAGTCACTTCTTTGTCGT
Reverse primer (PS-ApTCs)	TTGGTCGTGTCTAGGAACTAGGATA
Forward primer (p53)	GCTTTGAGGTGCGTGTTTG
Reverse primer (p53)	GTGAGGCTCCCCTTTCTTG
Forward primer (β-Actin)	ACCAACTGGGACGACATGGAGAAA
Reverse primer (β-Actin)	ATAGCACAGCCTGGATAGCAACG
FAM-modified DBCO-AS1411-PS (DBCO-AS1411-PS-FAM)	DBCO-T*T*G*G*T*G*G*T*G*G*T*G*G*T*T*G*T*G*G*T*G*G*T*G*G*T*G*T*G*G-FAM
Cy5-modified DBCO-AS1411-PS (DBCO-AS1411-PS-Cy5)	DBCO-T*T*G*G*T*G*G*T*G*G*T*G*G*T*T*G*T*G*G*T*G*G*T*G*G*T*G*T*G*G-Cy5
Cy5-modified DBCO-Random-PS (DBCO-Random-PS-Cy5)	DBCO-T*T*A*C*T*T*G*C*A*T*T*A*C*C*G*T*A*A*C*A*C*A*T*G*C*A*C*A-Cy5

[a]The asterisk indicate the bases were modified with phosphorothioate bonds.

Table S2. Pharmacokinetic (PK) parameters of PS-ApTCs in HeLa xenograft mouse model.[b]

PK parameter	mouse 1	mouse 2	mouse 3	mean ± SD
C_{max} (nM)	44.84	43.55	40.08	42.82 ± 2.46
AUC_{0-t} (nM*h)	159.77	162.07	168.93	163.59 ± 4.76
$AUC_{0-\infty}$ (nM*h)	163.45	166.62	169.69	166.59 ± 3.12
AUMC (nM*h^2)	568.58	712.76	729.12	670.15 ± 88.35
MRT (h)	3.56	4.40	4.32	4.09 ± 0.46
$t_{1/2}$ (h)	4.40	4.81	4.11	4.44 ± 0.35

[b]C_{max}: maximum plasma concentration. AUC_{0-t}: area under the concentration-time curve from time of injection (t=0) to a determined time point. $AUC_{0-\infty}$: area under the concentration-time curve from time of injection (t=0) to an infinite time point. AUMC: area under the first moment curve. MRT: mean residential time. $t_{1/2}$: terminal elimination half-life.

Uncropped full Western blot images

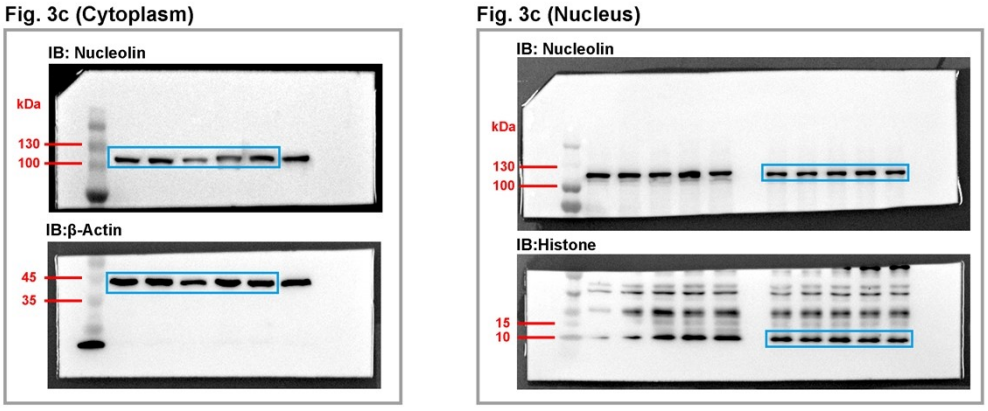

Uncropped full Western blot image of Fig. 3c. The samples derived from the same experiment, and the blots were processed in parallel. Loading controls, positive and negative controls, and molecular markers were all run on the same blot, with loading controls serving for normalization. The quantitation of protein expression represents relative protein level compared with the corresponding control after normalization with β-Actin or Histone (ImageJ software). The final western blotting images were obtained by overlaying the chemiluminescence image and the molecular weight markers image.

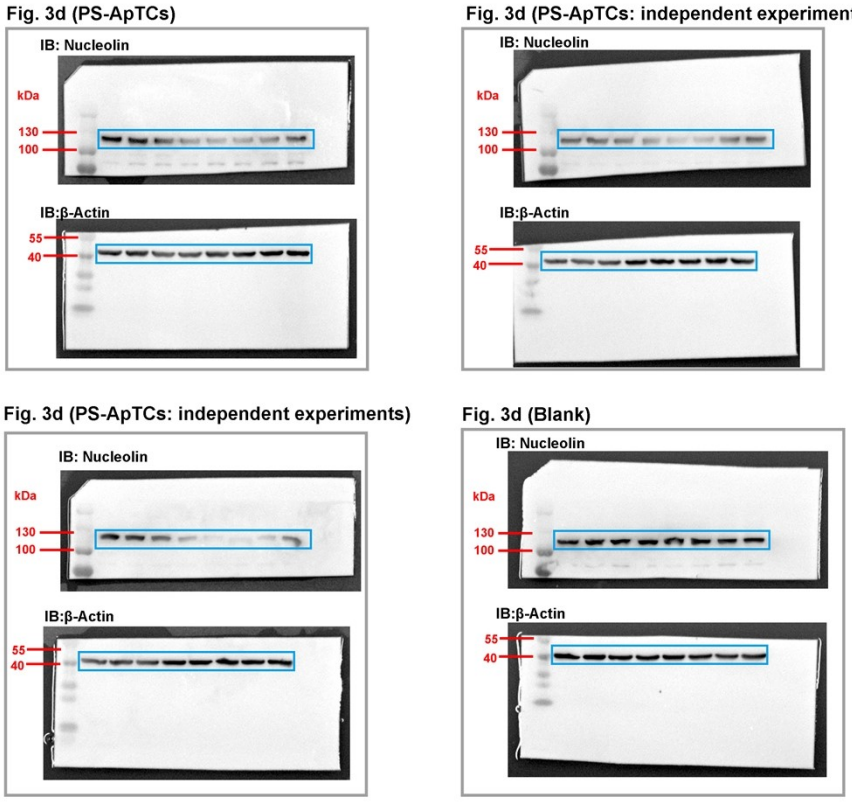

Uncropped full Western blot image of Fig. 3d. The samples derived from the same experiment, and the blots were processed in parallel. Loading controls, positive and negative controls, and molecular markers were all run on the same blot, with loading controls serving for normalization. The quantitation of protein expression represents relative protein level compared with the corresponding control after normalization with β-Actin (ImageJ software). The final western blotting images were obtained by overlaying the chemiluminescence image and the molecular weight markers image.

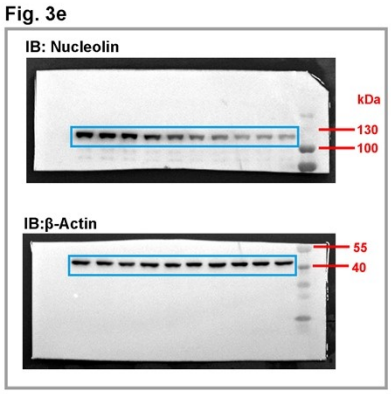

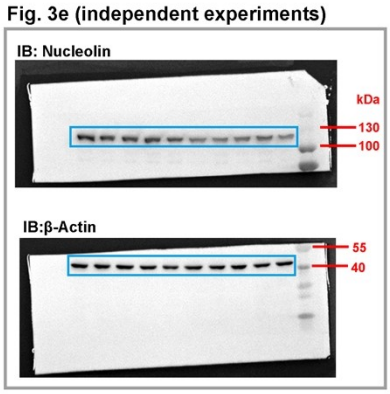

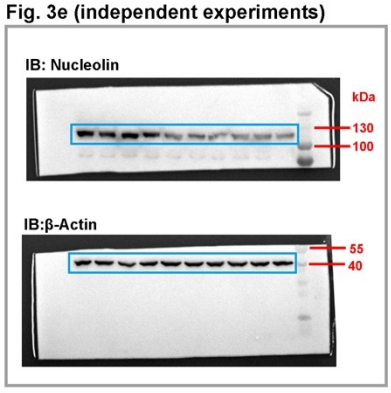

Uncropped full Western blot image of Fig. 3e. The samples derived from the same experiment, and the blots were processed in parallel. Loading controls, positive and negative controls, and molecular markers were all run on the same blot, with loading controls serving for normalization. The quantitation of protein expression represents relative protein level compared with the corresponding control after normalization with β-Actin (ImageJ software). The final western blotting images were obtained by overlaying the chemiluminescence image and the molecular weight markers image.

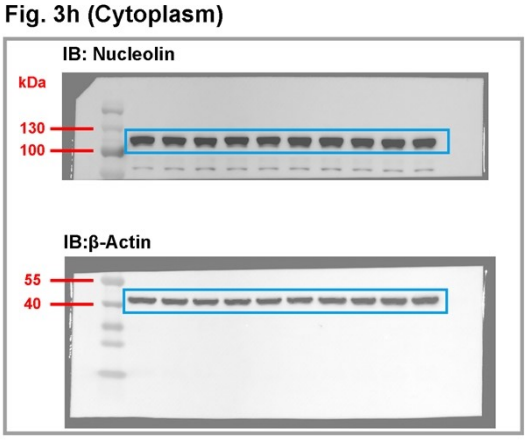

Uncropped full Western blot image of Fig. 3h. The samples derived from the same experiment, and the blots were processed in parallel. Loading controls, positive and negative controls, and molecular markers were all run on the same blot, with loading controls serving for normalization. The quantitation of protein expression represents relative protein level compared with the corresponding control after normalization with β-Actin (ImageJ software). The final western blotting images were obtained by overlaying the chemiluminescence image and the molecular weight markers image.

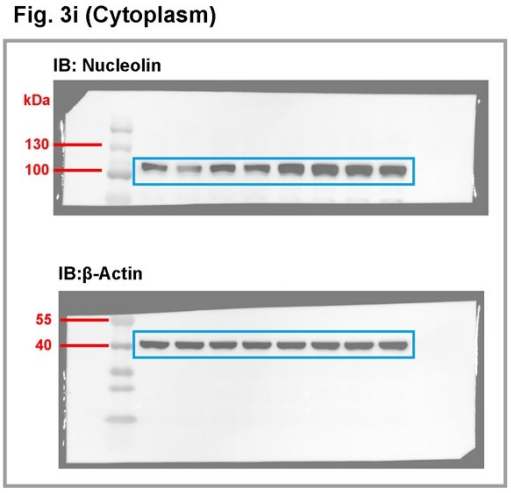

Uncropped full Western blot image of Fig. 3i. The samples derived from the same experiment, and the blots were processed in parallel. Loading controls, positive and negative controls, and molecular markers were all run on the same blot, with loading controls serving for normalization. The quantitation of protein expression represents relative protein level compared with the corresponding control after normalization with β-Actin (ImageJ software). The final western blotting images were obtained by overlaying the chemiluminescence image and the molecular weight markers image.

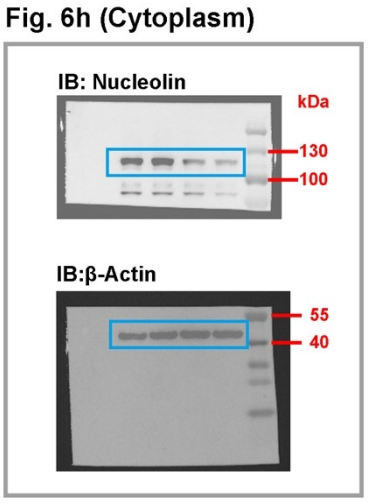

Uncropped full Western blot image of Fig. 6h. The samples derived from the same experiment, and the blots were processed in parallel. Loading controls, positive and negative controls, and molecular markers were all run on the same blot, with loading controls serving for normalization. The quantitation of protein expression represents relative protein level compared with the corresponding control after normalization with β-Actin (ImageJ software). The final western blotting images were obtained by overlaying the chemiluminescence image and the molecular weight markers image.

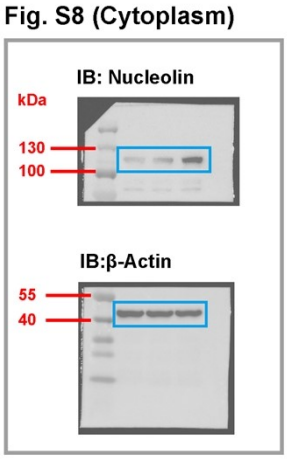

Uncropped full Western blot image of Fig. S8. The samples derived from the same experiment, and the blots were processed in parallel. Loading controls, positive and negative controls, and molecular markers were all run on the same blot, with loading controls serving for normalization. The quantitation of protein expression represents relative protein level compared with the corresponding control after normalization with β-Actin (ImageJ software). The final western blotting images were obtained by overlaying the chemiluminescence image and the molecular weight markers image.

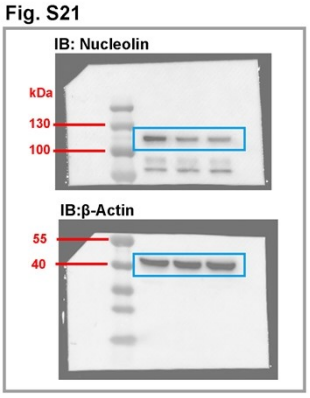

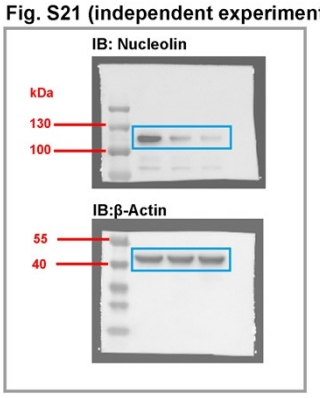

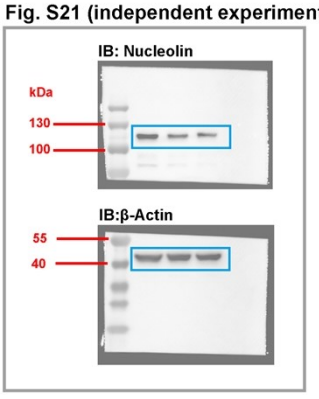

Uncropped full Western blot image of Fig. S21. The samples derived from the same experiment, and the blots were processed in parallel. Loading controls, positive and negative controls, and molecular markers were all run on the same blot, with loading controls serving for normalization. The quantitation of protein expression represents relative protein level compared with the corresponding control after normalization with β-Actin (ImageJ software). The final western blotting images were obtained by overlaying the chemiluminescence image and the molecular weight markers image.

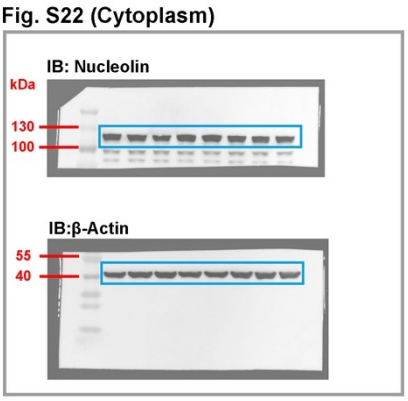

Uncropped full Western blot image of Fig. S22. The samples derived from the same experiment, and the blots were processed in parallel. Loading controls, positive and negative controls, and molecular markers were all run on the same blot, with loading controls serving for normalization. The quantitation of protein expression represents relative protein level compared with the corresponding control after normalization with β-Actin (ImageJ software). The final western blotting images were obtained by overlaying the chemiluminescence image and the molecular weight markers image.

Fig. S27 (Cytoplasm)

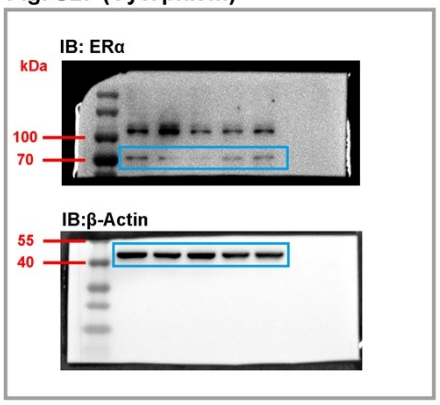

Uncropped full Western blot image of Fig. S27c. The samples derived from the same experiment, and the blots were processed in parallel. Loading controls, positive and negative controls, and molecular markers were all run on the same blot, with loading controls serving for normalization. The quantitation of protein expression represents relative protein level compared with the corresponding control after normalization with β-Actin (ImageJ software). The final western blotting images were obtained by overlaying the chemiluminescence image and the molecular weight markers image.

Fig. S29 (Cytoplasm)

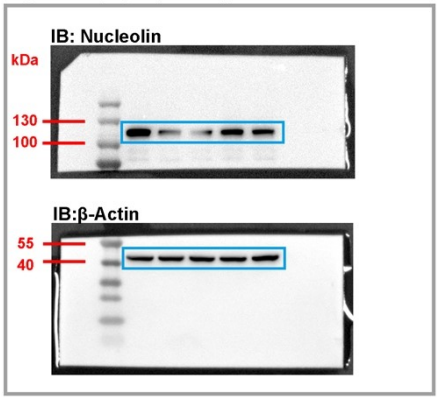

Uncropped full Western blot image of Fig. S29c. The samples derived from the same experiment, and the blots were processed in parallel. Loading controls, positive and negative controls, and molecular markers were all run on the same blot, with loading controls serving for normalization. The quantitation of protein expression represents relative protein level compared with the corresponding control after normalization with β-Actin (ImageJ software). The final western blotting images were obtained by overlaying the chemiluminescence image and the molecular weight markers image.

Fig. S32

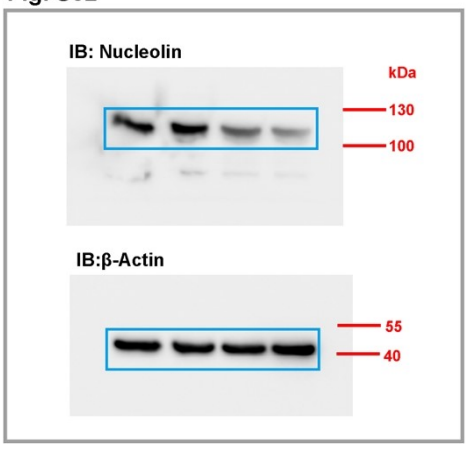

Uncropped full Western blot image of Fig. S32. The samples derived from the same experiment, and the blots were processed in parallel. Loading controls, positive and negative controls, and molecular markers were all run on the same blot, with loading controls serving for normalization. The quantitation of protein expression represents relative protein level compared with the corresponding control after normalization with β-Actin (ImageJ software).

Reference:

1 C. Steinebach, S. Lindner, N. D. Udeshi, D. C. Mani, H. Kehm, S. Kopff, S. A. Carr, M. Gutschow and J. Kronke, Homo-PROTACs for the Chemical Knockdown of Cereblon, *ACS Chem. Biol.*, 2018, **13**, 2771-2782.

2 J. Jang, C. To, D. J. H. De Clercq, E. Park, C. M. Ponthier, B. H. Shin, M. Mushajiang, R. P. Nowak, E. S. Fischer, M. J. Eck, P. A. Janne and N. S. Gray, Mutant-Selective Allosteric EGFR Degraders are Effective Against a Broad Range of Drug-Resistant Mutations, *Angew. Chem., Int. Ed.*, 2020, **59**, 14481-14489.

3 P. J. Boersema, R. Raijmakers, S. Lemeer, S. Mohammed and A. J. R. Heck, Multiplex Peptide Stable Isotope Dimethyl Labeling for Quantitative Proteomics, *Nat. Protoc.*, 2009, **4**, 484-494.

4 K. Han, E. E. Jeng, G. T. Hess, D. W. Morgens, A. Li and M. C. Bassik, Synergistic Drug Combinations for Cancer Identified in a CRISPR Screen for Pairwise Genetic Interactions, *Nat. Biotechnol.*, 2017, **35**, 463-474.